NASA TECHNICAL NOTE

NASA TN D-8514

NASA TN D-8514

COMPATIBILITY CHECK OF MEASURED AIRCRAFT RESPONSES USING KINEMATIC EQUATIONS AND EXTENDED KALMAN FILTER

Vladislav Klein and James R. Schiess

Langley Research Center
Hampton, Va. 23665

NATIONAL AERONAUTICS AND SPACE ADMINISTRATION • WASHINGTON D. C. • AUGUST 1977

COMPATIBILITY CHECK OF MEASURED AIRCRAFT RESPONSES USING KINEMATIC EQUATIONS AND EXTENDED KALMAN FILTER

Vladislav Klein* and James R. Schiess
Langley Research Center

SUMMARY

A process for the compatibility check of measured aircraft responses is presented. This process includes estimation of bias errors in the data and comparison of reconstructed responses with those measured directly. The model relating aircraft states and outputs is based on the six-degree-of-freedom kinematic equations and on output equations specifying the measured variables. Three model forms are presented. One of them includes the effect of atmospheric turbulence.

The estimation technique used is an extended Kalman filter with one-stage optimal smoothing. The algorithm also includes a time-varying process-noise covariance matrix, a fixed-point smoother, and an analysis of residuals.

The resulting technique is applied to simulated data to check the accuracy of the computing algorithm and the estimated bias errors. The compatibility check is also applied to measured flight data obtained from longitudinal and lateral maneuvers of a general aviation aircraft. Improved accuracy of measured data is obtained when the data are corrected for estimated bias errors.

INTRODUCTION

Estimation of aerodynamic characteristics of aircraft from flight data is receiving increased attention, partially because of the availability of sophisticated algorithms and computers for this purpose. In practice, it is found that biases or unknown scale factors are usually present in recorded data. Erroneous results for the aerodynamic characteristics are obtained and valuable research and computer time may be wasted before the researcher finds that the various data channels are not compatible. For example, data incompatibility would exist if the measured incidence angles did not agree with those reconstructed from the accelerometer and rate gyro measurements. A more efficient method for flight-test data analysis would be to determine first whether the data channels are all compatible, make whatever adjustments are required, and then use the refined "compatible data" for parameter estimation.

One of the first rigorous attempts of checking data compatibility was made in reference 1, in which the main objective was flight-path reconstruction from test data. Regression analysis and redundancy in measured data from three-

*The George Washington University, Joint Institute for Advancement of Flight Sciences.

degree-of-freedom longitudinal motion were used. This work was followed by reference 2, in which the aircraft states, constant biases in measured data, and initial conditions were estimated. The results were obtained from maximum likelihood estimation and an extended Kalman filter combined with fixed-interval smoothing. Later, using the latter technique, an extensive study of the same problem was made in reference 3.

A practical technique for obtaining the weighted least squares estimates of aircraft states, measurement biases, and initial conditions from measured data was introduced in reference 4. The mathematical model used was formed by the six-degree-of-freedom kinematic equations with measured accelerations and angular rates as input variables. The same model was used in reference 5, but the estimation algorithm was comprised of an extended Kalman filter-smoother and a fixed-point smoother. This technique was developed in reference 6 as "an advanced method" for identification of aircraft parameters and states.

The present report describes a computing procedure which

(1) Checks the consistency of the measured responses of an aircraft after removing the estimated bias errors in the measured data

(2) Reproduces some of the state variables and their first derivatives which are not measured directly

(3) Estimates the means, variances, autocorrelation functions, and power spectral densities of residuals

The model for the system to be analyzed is based on the aircraft six-degree-of-freedom kinematic equations and output equations specifying the measured variables. Three different models are considered. One of them includes the effect of atmospheric turbulence. This generalization has not been previously reported in the literature.

For estimation of aircraft states and bias errors, an extended Kalman filter from reference 6 was adopted. The algorithm was modified by introducing a time-varying process-noise covariance matrix and an analysis of residuals. The first modification, which extends the method of reference 6, improves the accuracy of the estimates in those cases where the process noise is nonstationary. The analysis of residuals should improve the filter performance by providing an indication for the selection of process- and measurement-noise covariance matrices. At the same time, the residuals give reasonable information about measurement-noise characteristics because the mathematical model used for the aircraft state estimation is, in general, very well defined.

The technique presented here should form part of a comprehensive process for the analysis of flight-test data and should precede any attempts at aircraft parameter estimation.

SYMBOLS

a_x, a_y, a_z	longitudinal, lateral, and vertical components of acceleration, m/sec^2
b_y	constant bias error in variable y
c_1, c_2	constants in differential equation for Gauss-Markoff process
D	matrix of dummy variables in fixed-point smoother algorithm
$E\{\ \}$	expected value
f	frequency, sec^{-1}
f( )	function which represents model
g	acceleration due to gravity, m/sec^2
H	$\partial h(\ )/\partial x^*$ evaluated along reference trajectory (see eq. (B2))
h	altitude, m
h( )	nonlinear output vector used to represent measurement system
I	identity matrix
K	Kalman filter gain
L	scale of turbulence, m
m	mean value of residuals
N	number of data points
n	measurement-noise vector
$n_1, n_2, \ldots, n_{16}$	elements of measurement-noise vector
P	covariance matrix of augmented state variables
p,q,r	roll, pitch, and yaw velocities, rad/sec or deg/sec
Q	process-noise covariance matrix
q_{jj}	jth main diagonal element of Q matrix
R	measurement-noise covariance matrix
$R_\nu(\tau)$	autocorrelation function of residuals ν
$S_\nu(f)$	power spectral density of residuals ν

$S(\omega)$	power spectral density of turbulence components
s	standard error estimate of residuals
t	time, sec
u,v,w	longitudinal, lateral, and vertical airspeed components, m/sec
u_g,v_g,w_g	longitudinal, lateral, and vertical turbulence velocity components, m/sec
V	true airspeed, m/sec
x	state vector
x^*	augmented state vector
x_b,y_b,z_b	linear position coordinates of aircraft, m
x_α,y_α	position coordinates of α_v wind vane with respect to aircraft cente of gravity, m
x_β,z_β	position coordinates of β_v wind vane with respect to aircraft cente of gravity, m
y	output vector
z	measurement vector
α_v	angle of attack measured by wind vane, rad or deg
β_v	sideslip angle measured by wind vane, rad or deg
$\delta(t),\delta_{ij}$	Kronecker delta for continuous and discrete data, respectively
η	input vector
Θ	vector of unknown parameters
θ	pitch angle, rad or deg
λ_y	scale factor error of variable y
ν_y	residual of variable y
ξ	process-noise vector
σ	standard error
σ^2	variance
τ	time lag, sec

Φ transition matrix for linearized equations

φ roll angle, rad or deg

ψ yaw angle, rad or deg

ω angular frequency, rad/sec

Subscripts:

E measured quantity

g gust

i index of data points

R uncorrected for bias errors

0 initial value

Superscript:

(j) index of iterations

Matrix exponents:

T transpose matrix

-1 inverse matrix

Mathematical Notation:

$\cdot$ over symbols denotes derivative with respect to time

$\hat{}$ over symbol denotes estimated value

Δ incremental value

A symbol followed by $(i|i)$ indicates the conditional mean or variance. For example, $\hat{x}(i-1|i)$ is the estimate of x_{i-1} based upon all measured data up to time t_i.

MATHEMATICAL MODEL RELATING AIRCRAFT STATES AND OUTPUTS

The mathematical model used for the data compatibility check is described, in general, by three sets of kinematic equations with the state variables consisting of three linear velocities u, v, and w; three position angles φ, θ, and ψ; and three linear positions x_b, y_b, and z_b. The input variables in the equations are the linear accelerations a_x, a_y, and a_z and angular rates p, q, and r. The kinematic equations (state equations) are formulated as

$$\dot{u} = -qw + rv + a_x - g \sin \theta \tag{1}$$

$$\dot{v} = -ru + pw + a_y + g \cos \theta \sin \varphi \tag{2}$$

$$\dot{w} = qu - pv + a_z + g \cos \theta \cos \varphi \tag{3}$$

$$\dot{\varphi} = p + q \sin \varphi \tan \theta + r \cos \varphi \tan \theta \tag{4}$$

$$\dot{\theta} = q \cos \varphi - r \sin \varphi \tag{5}$$

$$\dot{\psi} = q \sin \varphi / \cos \theta + r \cos \varphi / \cos \theta \tag{6}$$

$$\dot{x}_b = u \cos \theta \cos \psi + v(\sin \varphi \sin \theta \cos \psi - \cos \varphi \sin \psi) + w(\cos \varphi \sin \theta \cos \psi + \sin \varphi \sin \psi) \tag{7}$$

$$\dot{y}_b = u \cos \varphi \sin \psi + v(\sin \varphi \sin \theta \sin \psi + \cos \varphi \cos \psi) + w(\cos \varphi \sin \theta \sin \psi - \sin \varphi \cos \psi) \tag{8}$$

$$\dot{z}_b = -u \sin \theta + v \cos \theta \sin \varphi + w \cos \theta \cos \varphi \tag{9}$$

It is considered that the following variables are measured:

(1) The inputs to the system a_x, a_y, a_z, p, q, and r

(2) The airspeed V, two incidence angles β_v and α_v, three position angles φ, θ, and ψ, and altitude $h = -z_b$ (these variables represent the output of the system)

The measured variables z are corrupted by systematic and random errors. It is, therefore, assumed that each can be expressed as

$$z = (1 + \lambda_y)y + b_y + n \tag{10}$$

where y is the true value of the output, λ_y is the unknown scale factor, b_y is the constant bias error, and n is the measurements noise. It is further assumed that the scale factor λ_y is nonzero only for variables V, β_v, and α_v which are directly connected with airflow measurement.

In flight-test experiments, the horizontal and lateral positions of an aircraft with respect to a given point on the ground are usually neither measured nor requested. For that reason, the system of state equations can be simplified by deleting equations (7) and (8). Then, replacing the input variables in

the remaining state equations by their measured values results in a new set of state equations as follows:

$$\begin{bmatrix}\dot{u}\\ \dot{v}\\ \dot{w}\\ \dot{h}\end{bmatrix} = \begin{bmatrix} 0 & r_{R,E} - b_r & -(q_{R,E} - b_q) & 0 \\ -(r_{R,E} - b_r) & 0 & p_{R,E} - b_p & 0 \\ q_{R,E} - b_q & -(p_{R,E} - b_p) & 0 & 0 \\ \sin\theta & -\cos\theta \sin\varphi & -\cos\theta \cos\varphi & 0 \end{bmatrix} \begin{bmatrix} u \\ v \\ w \\ h \end{bmatrix}$$

$$+ \begin{bmatrix} -g \sin\theta \\ g \cos\theta \sin\varphi \\ g \cos\theta \cos\varphi \\ 0 \end{bmatrix} + \begin{bmatrix} a_{x,R,E} \\ a_{y,R,E} \\ a_{z,R,E} \\ 0 \end{bmatrix} + \begin{bmatrix} -b_{ax} \\ -b_{ay} \\ -b_{az} \\ 0 \end{bmatrix} + \begin{bmatrix} 0 & w & -v & 0 \\ -w & 0 & u & 0 \\ v & -u & 0 & 0 \\ 0 & 0 & 0 & 0 \end{bmatrix} \begin{bmatrix} n_4 \\ n_5 \\ n_6 \\ 0 \end{bmatrix} + \begin{bmatrix} n_1 \\ n_2 \\ n_3 \\ 0 \end{bmatrix} \tag{11a}$$

$$\begin{bmatrix}\dot{\varphi}\\ \dot{\theta}\\ \dot{\psi}\end{bmatrix} = \begin{bmatrix} 1 & \sin\varphi \tan\theta & \cos\varphi \tan\theta \\ 0 & \cos\varphi & -\sin\varphi \\ 0 & \sin\varphi/\cos\theta & \cos\varphi/\cos\theta \end{bmatrix} \begin{bmatrix} p_{R,E} - b_p + n_4 \\ q_{R,E} - b_q + n_5 \\ r_{R,E} - b_r + n_6 \end{bmatrix} \tag{11b}$$

The output equations take the form

$$\left.\begin{aligned} V_R &= (1 + \lambda_V)\sqrt{u^2 + v^2 + w^2} + b_V \\ \beta_{v,R} &= (1 + \lambda_\beta) \tan^{-1}\left[\frac{v + (r_{R,E} - b_r)x_\beta - (p_{R,E} - b_p)z_\beta}{u}\right] + b_\beta \\ \alpha_{v,R} &= (1 + \lambda_\alpha) \tan^{-1}\left[\frac{w - (q_{R,E} - b_q)x_\alpha + (p_{R,E} - b_p)y_\alpha}{u}\right] + b_\alpha \\ \varphi_R &= \varphi + b_\varphi \\ \theta_R &= \theta + b_\theta \\ \psi_R &= \psi + b_\psi \\ h_R &= h + b_h \end{aligned}\right\} \tag{12}$$

where b_y are the constant bias errors in the input and output variables. Equations (11) and (12) are similar to those developed and used in reference 5.

In formulating the output equations for $\beta_{v,R}$ and $\alpha_{v,R}$, the effect of random errors in p, q, and r was neglected. The output equations also do not include the effect of atmospheric disturbances. Therefore, it is further assumed that all flight data are obtained from measurement in still air. However, a gust disturbance model which can be incorporated into the analysis is presented in a subsequent section.

The measured values in the state equations introduce process noise into the system and make the system model stochastic. The process noise in equations (11) is nonstationary and cross-correlated. Two assumptions are made concerning the process noise:

(a) All cross-correlations between process-noise components are neglected.

(b) The process noise has zero mean value and its covariance matrix varies with time. The expressions for the elements of the covariance matrix are given in appendix A.

The general form of the state equation for the given system can be written as

$$\dot{x} = f(x,\eta,\Theta,t) + \xi(t) \tag{13}$$

and the discrete form of the measurement equation as

$$z_i = h_i(x_i,\eta_i,\Theta) + n_i \qquad (i = 0,1,\ldots,N) \tag{14}$$

where x is the state vector, η is the input vector, z is the measurement vector, $\Theta^T = [b_y,\lambda_y]$ is the vector of unknown parameters, $\xi(t)$ is the process-noise vector with $E\{\xi(t)\} = 0$ and $E\{\xi(t)\,\xi^T(\tau)\} = Q(t)\,\delta(t-\tau)$, n_i is the measurement-noise vector with $E\{n_i\} = 0$, and $E\{n_i n_j^T\} = R\delta_{ij}$, and N is the number of data points. The matrices $Q(t)$ and R are the covariance matrices for the process and measurement noise, respectively, the first one being time dependent and the other constant.

Model With Measured Angular Accelerations

In some cases, the angular accelerations $\dot{p}$, $\dot{q}$, and $\dot{r}$ can also be obtained from measurement. When substituted into the system model equations, these accelerations form the input variables, and the angular rates become outputs of the system. The state equations are changed as follows:

$$\begin{bmatrix}\dot{u}\\ \dot{v}\\ \dot{w}\\ \dot{h}\end{bmatrix} = \begin{bmatrix} 0 & r & -q & 0\\ -r & 0 & p & 0\\ q & -p & 0 & 0\\ \sin\theta & -\cos\theta\sin\varphi & -\cos\theta\cos\varphi & 0\end{bmatrix}\begin{bmatrix}u\\ v\\ w\\ h\end{bmatrix} + \begin{bmatrix} -g\sin\theta\\ g\cos\theta\sin\varphi\\ g\cos\theta\cos\varphi\\ 0\end{bmatrix}$$

$$+ \begin{bmatrix} a_{x,R,E} - b_{ax} + n_1\\ a_{y,R,E} - b_{ay} + n_2\\ a_{z,R,E} - b_{az} + n_3\\ 0\end{bmatrix} \qquad (15a)$$

$$\begin{bmatrix}\dot{p}\\ \dot{q}\\ \dot{r}\end{bmatrix} = \begin{bmatrix}\dot{p}_{R,E} - b_{\dot{p}} + n_{14}\\ \dot{q}_{R,E} - b_{\dot{q}} + n_{15}\\ \dot{r}_{R,E} - b_{\dot{r}} + n_{16}\end{bmatrix} \qquad (15b)$$

$$\begin{bmatrix}\dot{\varphi}\\ \dot{\theta}\\ \dot{\psi}\end{bmatrix} = \begin{bmatrix}1 & \sin\varphi\tan\theta & \cos\varphi\tan\theta\\ 0 & \cos\varphi & -\sin\varphi\\ 0 & \sin\varphi/\cos\theta & \cos\varphi/\cos\theta\end{bmatrix}\begin{bmatrix}p\\ q\\ r\end{bmatrix} \qquad (15c)$$

where $b_{\dot{p}}$, $b_{\dot{q}}$, and $b_{\dot{r}}$ are the constant bias errors in the angular accelerations. Output equations (12) are completed by three equations:

$$p_R = p + b_p$$

$$q_R = q + b_q$$

$$r_R = r + b_r$$

In equations (15), the process noise enters explicitly and can be considered stationary. Additional measurements of angular accelerations provide possibilities for estimating the measurement-noise characteristics of angular velocities and also the process-noise characteristics, as explained in reference 6.

Model With Gust Disturbances

In general, gusts can be taken into account by modeling the spectra of atmospheric turbulence. The model is based on the assumption that the turbulence field is steady and homogeneous. By using Dryden's model (see, e.g., ref. 7, pp. 315-318), the power spectral densities of the horizontal, lateral, and vertical turbulence velocity components are represented by

$$S_{ug}(\omega) = \sigma_{ug}^2 \frac{2L_u}{\pi} \frac{1}{1 + \left(L_u \frac{\omega}{V}\right)^2} \tag{16}$$

$$S_{vg}(\omega) = \sigma_{vg}^2 \frac{L_v}{\pi} \frac{1 + 3\left(L_v \frac{\omega}{V}\right)^2}{\left[1 + \left(L_v \frac{\omega}{V}\right)^2\right]^2} \tag{17}$$

$$S_{wg}(\omega) = \sigma_{wg}^2 \frac{L_w}{\pi} \frac{1 + 3\left(L_w \frac{\omega}{V}\right)^2}{\left[1 + \left(L_w \frac{\omega}{V}\right)^2\right]^2} \tag{18}$$

where L_u, L_v, and L_w are the scales of turbulence and σ_{ug}^2, σ_{vg}^2, and σ_{wg}^2 are the variances of the turbulence velocity components. It is also assumed that the turbulence field is isotropic; therefore,

$$L_u = L_v = L_w = L$$

$$\sigma_{ug}^2 = \sigma_{vg}^2 = \sigma_{wg}^2 = \sigma_g^2$$

For further simplification of the turbulence modeling, equations (17) and (18) can be approximated by

$$S_{vg}(\omega) = S_{wg}(\omega) = \sigma_g^2 \frac{3L}{2\pi} \frac{1}{1 + \left(\frac{L}{\sqrt{2}} \frac{\omega}{V}\right)^2} \tag{19}$$

Turbulence with the power spectral density given by equation (16) or (19) can be described as a Gauss-Markoff process of first order. The corresponding differential equation is given as

$$\dot{x}_g = -c_1 x_g + c_2 n_g \tag{20}$$

where x_g is a turbulence velocity component u_g, v_g, or w_g and n_g represents a normally distributed white noise with zero mean and variance σ_g^2. The constants c_1 and c_2 have the form for horizontal gust,

$$c_1 = \frac{V}{L} \qquad c_2 = V\sqrt{\frac{2}{\pi L}}$$

and the lateral and vertical gust,

$$c_1 = \sqrt{2\,\frac{V}{L}} \qquad c_2 = V\sqrt{\frac{3}{\pi L}}$$

The only measurements which the gust affects directly are airspeed, sideslip angle, and angle of attack. The perturbations due to gust on these variables may be expressed as

$$\left.\begin{aligned} V_g &\approx u_g \\ \beta_g &\approx \frac{v_g}{u} \\ \alpha_g &\approx \frac{w_g}{u} \end{aligned}\right\} \tag{21}$$

With the gust disturbances taken into account, state equations (11) or (15) can be extended by three equations for u_g, v_g, and w_g based on equation (20). The first three output equations can be modified to

$$V_R = (1 + \lambda_V)\left(\sqrt{u^2 + v^2 + w^2} - u_g\right) + b_V$$

$$\beta_{v,R} = (1 + \lambda_\beta)\,\tan^{-1}\left[\frac{v + (r_{R,E} - b_r)x_\beta - (p_{R,E} - b_p)z_\beta}{u} - \frac{v_g}{u}\right] + b_\beta$$

$$\alpha_{v,R} = (1 + \lambda_\alpha)\,\tan^{-1}\left[\frac{w - (q_{R,E} - b_q)x_\alpha + (p_{R,E} - b_p)y_\alpha}{u} - \frac{w_g}{u}\right] + b_\alpha$$

For the solution of the extended system of state equations, the values of L and σ_g^2 must be given. A good approximation for the scale of turbulence is $L = 300$. A rough estimate of σ_g^2 can be obtained from the random component of the recorded wind-vane reading.

IDENTIFICATION TECHNIQUE

By using the extended Kalman filter, identification of the system given by equations (13) and (14) can be achieved as the state estimation of a nonlinear system with the augmented state vector

$$x^* = \begin{bmatrix} x \\ -- \\ \Theta \end{bmatrix} \tag{22}$$

Because of augmenting the state vector with the unknown parameter vector, state equation (13) is changed to

$$\dot{x}^* = \begin{bmatrix} f(x,\eta,\Theta,t) \\ \hline 0 \end{bmatrix} + \begin{bmatrix} \xi(t) \\ \hline 0 \end{bmatrix} \tag{23}$$

The algorithm is obtained by linearizing the system and measurement equations around the best estimate of states at each data point. In order to correct for system and measurement nonlinearities, the computing algorithm presented in reference 5 includes "local iteration" and one-stage optimal smoothing. At time t_{i-1}, the algorithm starts with $\hat{x}^{*(j)}(i-1|i-1)$ and $P^{(j)}(i-1|i-1)$, where the exponent j indicates the jth iteration. Then the algorithm predicts and updates states and state variances to time t_i by applying one iteration of the extended filter. Finally, on the basis of this new estimate, it smooths back to t_{i-1}. The smoothing closes the loop to provide an improved reference for the new prediction at t_i. The iteration terminates when there is no significant difference between consecutive iterations or after a specific number of iterations. Analysis in reference 6 showed that this procedure can significantly reduce the bias which is inherent in the extended Kalman filter. The computing scheme for one stage with two iterations is presented in figure 1.

At each data point the extended Kalman filter provides the information for the fixed-point smoother. The basic feature of the algorithm is that no storage for the filtered states and state covariance matrices is required. The algorithm works in conjunction with the extended Kalman filter. After each step from t_{i-1} to t_i, the smoother computes the smoothed estimates $\hat{x}^*(0|i)$ and $P(0|i)$, thus ending with $\hat{x}^*(0|N)$ and $P(0|N)$ when all data are processed.

The algorithm for the locally iterated extended Kalman filter combined with the fixed-point smoother is summarized in appendix B. The schematic block diagram for the identification technique indicating initial data required and results obtained is given in figure 2.

ANALYSIS OF RESIDUALS

Residuals are defined as the differences between measured variables and their predicted values:

$$\nu_i = z_i - \hat{y}(i|i-1) \tag{24}$$

For the correct values of the process-noise and measurement-noise covariance matrices and the correct model of the system, the residuals should approach a random Gaussian, white sequence with zero mean. The variances should be consistent with calculated values from filter equation (B5); that is,

$$E\left\{\nu_i^{(j)} \nu_i^{(j)T}\right\} = H_i^{(j)} P^{(j)}(i|i-1) H_i^{(j)T} + R \tag{25}$$

Because of its presence in equation (B4), the process-noise covariance matrix influences the predicted state covariance matrix. Therefore, equation (25) can be used for the consistency check between the matrices Q_i and R and the time histories of residuals, provided that the model defined by equations (23) and (14) is correct. The plotted residuals should be within the boundaries given by the square root of the main diagonal elements in the matrix defined by equation (25). If the boundaries are either too large or too small, the matrices Q_i and R which are not known a priori and must therefore be estimated in advance, should be adjusted accordingly.

The mathematical model of the system is based on the general form of the aircraft kinematic equations. The uncertainty in the model used is in the form of the measurement equation (10), where only constant bias errors are considered. Despite this uncertainty, the assumption of negligible modeling errors can be substantiated. Then, with good estimates for Q_i and R, the residuals reflect the characteristics of the measurement-noise components, mainly the frequency contents in their power spectral densities.

For these reasons mentioned, the extended Kalman filter-smoother has been complemented by the analysis of residuals. From their time histories, the mean values, variances, autocorrelation functions, and power spectral densities of the residuals are estimated. For the estimates of the autocorrelation functions and power spectral densities, the expressions from reference 8 (pp. 290-295) were used.

EXAMPLES USING SIMULATED DATA

The data consistency check procedure developed in the present study was applied to simulated data to check the accuracy of the computing algorithm and the estimated bias errors. Simulated data used represent the six-degree-of-freedom maneuvers of an aircraft. A summary of the measured variables and standard errors of the simulated measurement noise is given in table I. In table II, the elements of the augmented state vector and the initial estimates of their variances are presented. The number of data points is $N = 400$ and the time interval is $\Delta t = 0.05$ sec.

First the simulated data were used to evaluate the effect of varying the number of terms in the transition matrix (eq. (B1)) and the number of iterations in the single-stage smoother. As a result, six terms of the Taylor series expansion were used for the approximation of the state transition matrix, and the number of iterations in the single-stage smoother was set equal to two.

The effect of using a time-dependent or constant process-noise covariance matrix was also investigated. The initial estimates

$$\Theta_0^T = \left[b_y, \lambda_y\right]$$

and $\hat{x}^*(0|0)$ were set equal to their true values, and two cases were computed. Results are given in table III. In case 1 the Q matrix was kept constant; that is, $Q_i = Q_0$ for all i. In case 2 the Q matrix varied with time as expressed by equations (A3). Comparison of results shows improved accuracy of

the parameter estimates in case 2, although their standard errors (lower bounds) presented in parentheses are larger than those in case 1. It was therefore decided to include equations (A3) in the algorithm. Similar procedures in references 2, 3, and 4 use a constant approximation for the Q matrix.

In table IV the effect of unknown initial values for the parameter estimates and their variances and the number of unknown parameters is demonstrated. For case 3, the data were processed five times. The initial estimates of the unknown parameters were first set equal to zero. Then, in the following four passes, they were always updated with the final estimates from the previous pass. For several parameters, improved accuracy of the estimates after five passes is apparent. This example also shows the small effect of the initial values $P(0|0)$ on the final estimates $P(N|N)$. In case 4 the number of unknown parameters was reduced from 14 to 6. The new set of unknown parameters was connected with variables defining the lateral motion of an aircraft. The initial parameter estimates were again set equal to zero. The decreased number of unknowns resulted in better accuracy of the estimates, although it was not possible to estimate the parameter λ_β more accurately. This was caused by the low sensitivity of the output variables to the parameter λ_β as indicated by its standard error.

ANALYSIS OF MEASURED FLIGHT DATA

Flight-test data were obtained on a small single-engine general aviation aircraft. The first run analyzed represents longitudinal motion of the aircraft excited by elevator deflection. In the second example, measurements were available from eight runs using rudder and aileron deflections as input. For these runs, flight conditions were the same; only the forms of both inputs were different. The use of large amplitudes of rudder and aileron deflection resulted in coupling between the lateral and the longitudinal motion of the aircraft.

Three-Degree-of-Freedom Longitudinal Motion

The model for the extended Kalman filter-smoother included the following state, input, and output variables:

$$x^T = \left[u, w, \theta\right]$$

$$\eta^T = \left[a_{x,R,E}, a_{z,R,E}, q_{R,E}\right]$$

$$y^T = \left[V_R, \alpha_{v,R}, \theta_R\right]$$

The vector of unknown parameters was assumed in the form

$$\Theta^T = \left[b_{ax}, b_{az}, b_q, b_V, b_\alpha, b_\theta, \lambda_V, \lambda_\alpha\right]$$

The time histories of measured input and output variables are plotted in figure 3. For the measured data, the sampling interval was $\Delta t = 0.1$ sec and the

number of data points was N = 198. The estimated parameters, standard errors, and sensitivities from the three computer passes are given in table V. In the first pass, the initial values of the parameters were set equal to zero and the initial variances were set equal to those given in table VI. Then, in the following passes, the initial values were always equal to the final fixed-point smoother estimates from the preceding pass. Results from the first and third passes show some changes in parameters and slightly improved accuracy of the final estimates. The accuracy is expressed as the Cramer-Rao lower bound on the standard error of the estimates. These values are given in parentheses.

Some of the estimated parameters have high standard error which can be due to their small significance in the model. In order to investigate this possibility, the sensitivities of the output variables with respect to the unknown parameters were computed. The expression for the sensitivity was taken from reference 9 as $\Theta_j^2 P_{jj}^{-1}$, where P_{jj}^{-1} is the main diagonal element of the information matrix $P^{-1}(N|N)$. The computed sensitivities are also presented in table V.

In the fourth pass the parameters b_{az}, b_q, and b_θ with high uncertainty and small sensitivity were fixed at their last estimated values. The resulting estimates of remaining parameters were more accurate and had more uniform sensitivities than those from the complete model.

For all passes the initial values of the process-noise covariance matrix Q_0 were the same. The initial values of the measurement-noise covariance matrix were changed by comparing their values with the estimates $P(0|N)$ for the state variables and with the variances of the residuals.

The time histories of the parameters from the fourth pass are shown in figure 4. With the exception of b_{ax}, they do not indicate any substantial changes toward the end of the time interval. The corresponding variances were almost constant within the whole time interval.

In table VI the initial values of the state variables and variances from two passes are compared with the smoothed values. There is only slightly better agreement between these values after two passes.

The measured and predicted output time histories are plotted in figure 5, and the residuals in figure 6. The 2σ bounds in the residual plots were estimated from equation (25). The agreement between measured and reconstructed responses indicates good data compatibility. Because almost all residuals for each variable are within 2σ bounds, reasonable initial values for the matrices R and Q_0 can be expected. The outputs from the deterministic model based on equations (1) to (5) were also computed and compared with measurements in figure 7. The resulting errors are given in figure 8. The errors in the deterministic model are quite large in all variables, especially in α_v. The main reason might be due to neutrally stable modes in the deterministic model.

The analysis of residuals is summarized in figures 9 and 10, where the mean values, standard errors, autocorrelation functions, and power spectral densities of residuals are presented. From figures 9 and 10, it is apparent that only the

residuals in the pitch angle are close to the random white sequence. The residuals in the remaining two variables are distorted by deterministic components of an unknown origin.

Six-Degree-of-Freedom Motion

The compatibility check was also applied to measurements from eight runs in which large-amplitude rudder and aileron deflection resulted in coupling between the lateral and longitudinal motion of the aircraft. The sampling interval for the measured data was $\Delta t = 0.05$ sec; the number of measured data points was $N = 200$ for the first four runs and $N = 400$ for the remaining runs. The state, input, and output vectors were defined as

$$x^T = \left[u, v, w, \varphi, \theta\right]$$

$$\eta^T = \left[a_{x,R,E}, a_{y,R,E}, a_{z,R,E}, p_E, q_E, r_E\right]$$

$$y^T = \left[V_R, \beta_{v,R}, \alpha_{v,R}, \varphi_R, \theta_R\right]$$

In the first pass the vector of unknown parameters had 12 elements. After the uncertainty and sensitivity of all the estimated parameters were examined, the number of unknowns was reduced by two and the vector Θ was formed as

$$\Theta^T = \left[b_{ax}, b_{ay}, b_{az}, b_r, b_\beta, b_\alpha, b_\varphi, b_\theta, \lambda_\gamma, \lambda_\beta\right]$$

The estimated parameters from eight runs are presented in table VII. The standard errors of the same parameters differed little between runs. Therefore, only the average values of these standard errors from all eight runs are included. For some parameters, the estimates are quite consistent. The largest inconsistency was observed in the bias error for the sideslip angle.

The comparison of the measured and predicted outputs for run 5 is given in figure 11. The comparison of measured and reconstructed variables is good. Similar agreements were observed in the remaining runs. The residuals from run 5 are plotted in figure 12, and the autocorrelation functions in figure 13. As for three-degree-of-freedom longitudinal motion, the residuals in some variables indicate the presence of deterministic components.

CONCLUDING REMARKS

A process for the compatibility check of measured aircraft responses has been presented. This process includes the estimation of bias errors in the data and comparison of some reconstructed responses with those measured directly. The model relating aircraft states and outputs is based on the six-degree-of-freedom kinematic equations and on output equations specifying the measured variables. Three model forms are presented, one of which includes the effect of atmospheric turbulence.

The estimation technique used was an extended Kalman filter with one-stage optimal smoothing. Application of this smoothing can significantly reduce the bias which is inherent in the extended Kalman filter. In order to further improve the accuracy of the estimates, the algorithm includes a time-varying process-noise covariance matrix, a fixed-point smoother, and an analysis of residuals. The smoother gives smoothed initial estimates of states, parameters, and their covariance matrix. The analysis of residuals can help to verify the preselected values of the process- and measurement-noise covariance matrices by comparing the residual variances obtained from the filter with those from the time histories of residuals. In addition, it provides estimates of characteristics of the measurement noise in terms of the autocorrelation functions or power spectral densities.

The resulting technique was first applied to simulated data to check the accuracy of the computing algorithm and the estimated bias errors. It was shown that the replacement of a constant process-noise covariance matrix with the time-variable one can improve the estimates where the process noise is nonstationary.

The accuracy of the estimates was also improved by iteratively processing the data several times. The reprocessing used the final estimates from the previous pass as the new initial estimates for parameters.

The compatibility check was also applied to measured flight data. In the first example the data from longitudinal motion were analyzed. The covariance matrix of the states and parameters and the inverse of this matrix, were used for the assessment of the relative accuracy of the estimates and the sensitivity of the model outputs with respect to unknown parameters. Then, in the repeated pass, parameters with very small accuracy and sensitivity were dropped from the model. This simplification of the model resulted in improved accuracy of the remaining parameters.

The second example included a compatibility check of the lateral responses of an aircraft in eight repeated runs. The repeatability of estimates obtained was good even when model included 5 states and 10 parameters.

The estimated autocorrelation functions and power spectral densities of residuals in both examples show that in some cases the estimated measurement-noise characteristics may be different from those assumed for white noise. The reason for this discrepancy might be any remaining unknown deterministic components in the measured data.

National Aeronautics and Space Administration
Langley Research Center
Hampton, VA 23665
June 14, 1977

APPENDIX A

PROCESS-NOISE COVARIANCE MATRIX

The process-noise vector in state equation (23) has the form

$$\begin{bmatrix} \xi_1 \\ -- \\ \xi_2 \\ -- \\ 0 \end{bmatrix}$$

where

$$\xi_1 = \begin{bmatrix} 0 & w & -v & 0 \\ -w & 0 & u & 0 \\ v & -u & 0 & 0 \\ 0 & 0 & 0 & 0 \end{bmatrix} \begin{bmatrix} n_4 \\ n_5 \\ n_6 \\ 0 \end{bmatrix} + \begin{bmatrix} n_1 \\ n_2 \\ n_3 \\ 0 \end{bmatrix} \tag{A1}$$

$$\xi_2 = \begin{bmatrix} 1 & \sin\varphi \tan\theta & \cos\varphi \tan\theta \\ 0 & \cos\varphi & -\sin\varphi \\ 0 & \sin\varphi/\cos\theta & \cos\varphi/\cos\theta \end{bmatrix} \begin{bmatrix} n_4 \\ n_5 \\ n_6 \end{bmatrix} \tag{A2}$$

By using equations (A1) and (A2) and the assumption of no correlation between the measurement-noise components, the main diagonal elements of the process-noise covariance matrix can be expressed as

$$\left.\begin{aligned} q_{11} &= \sigma_1^2 + w^2\sigma_5^2 + v^2\sigma_6^2 \\ q_{22} &= \sigma_2^2 + w^2\sigma_4^2 + u^2\sigma_6^2 \\ q_{33} &= \sigma_3^2 + v^2\sigma_4^2 + u^2\sigma_5^2 \\ q_{44} &= 0 \\ q_{55} &= \sigma_4^2 + (\sin\varphi \tan\theta)^2\sigma_5^2 + (\cos\varphi \tan\theta)^2\sigma_6^2 \\ q_{66} &= \cos^2\varphi\,\sigma_5^2 + \sin^2\varphi\,\sigma_6^2 \\ q_{77} &= (\sin\varphi/\cos\theta)^2\sigma_5^2 + (\cos\varphi/\cos\theta)^2\sigma_6^2 \\ q_{88} &= q_{99} = \ldots = q_{23\,23} = 0 \end{aligned}\right\} \tag{A3}$$

where σ_j^2 is the variance of the measurement noise n_j for $j = 1,2,\ldots,6$.

APPENDIX A

Equations (A3) can be simplified by replacing the time variables $u, v, \ldots, (\cos\varphi/\cos\theta)$ by their average values which depend upon the flight record being analyzed.

APPENDIX B

EXTENDED KALMAN FILTER-SMOOTHER AND FIXED-POINT SMOOTHER

In the algorithm from reference 5 for an extended Kalman filter-smoother, the following notation is introduced:

$$\Phi^{(j)}(i,i-1) = \left[I + \frac{\partial f}{\partial x} \Delta t + \frac{1}{2}\left(\frac{\partial f}{\partial x^*}\right)^2 \Delta t^2 + \ldots \right]\Bigg|_{\hat{x}^{*(j)}(i-1|i)} \tag{B1}$$

$$H_i^{(j)} = \frac{\partial h\left[\hat{x}^{*(j)}(i|i)\right]}{\partial x^*} \tag{B2}$$

$$\nu_i^{(j)} = z_i - h_i\left[\hat{x}^{*(j)}(i|i)\right] - H_i^{(j)}\left[\hat{x}^{*(j)}(i|i-1) - \hat{x}^{*(j)}(i|i)\right]$$

$$\Delta t = t_i - t_{i-1}$$

Before the computing starts, it is necessary to set $i = 1$, $j = 1$, and $\hat{x}^{*(1)}(i-1|i) = \hat{x}^{*}(i-1|i-1)$. Then the filter-smoother proceeds in the following steps:

(1) State prediction

$$\hat{x}^{*(j)}(i|i-1) = \int_{t_{i-1}}^{t_i} f(\hat{x}^*,\eta,t)\, dt + \Phi^{(j)}(i,i-1)\left[\hat{x}^{*}(i-1|i-1) - \hat{x}^{*(j)}(i-1|i)\right] \tag{B3}$$

If $j = 1$, set $\hat{x}^{*(j)}(i|i) = \hat{x}^{*(j)}(i|i-1)$

(2) State covariance prediction

$$P^{(j)}(i|i-1) = \Phi^{(j)}(i,i-1)\, P(i-1|i-1)\, \Phi^{(j)T}(i,i-1) + Q_i \tag{B4}$$

(3) Gain estimation

$$K_i^{(j)} = P^{(j)}(i|i-1)\, H_i^{(j)T}\left[H_i^{(j)}\, P^{(j)}(i|i-1)\, H_i^{(j)T} + R\right]^{-1} \tag{B5}$$

(4) State updating

$$\hat{x}^{*(j+1)}(i|i) = \hat{x}^{*(j)}(i|i-1) + K_i^{(j)}\nu_i^{(j)} \tag{B6}$$

(5) State covariance updating

$$P^{(j)}(i|i) = \left(I - K_i^{(j)}H_i^{(j)}\right)P^{(j)}(i|i-1) \tag{B7}$$

(6) State smoothing

$$\hat{x}^{*(j+1)}(i-1|i) = \hat{x}^{*}(i-1|i-1) + P(i-1|i-1)\,\Phi^{(j)T}(i,i-1)\,H_i^{(j)T}$$

$$\times \left[H_i^{(j)}\,P^{(j)}(i|i-1)\,H_i^{(j)T} + R\right]^{-1} \nu_i^{(j)} \qquad \text{(B8)}$$

When the first iteration is completed, j is incremented and the filter-smoother starts again with equation (B3). If $\hat{x}^{*(j)}(i|i) \approx \hat{x}^{*(j+1)}(i|i)$ or $j = j_{max}$ which is the specified number of iterations, then $\hat{x}^{*}(i|i)$ is set equal to $\hat{x}^{*(j+1)}(i|i)$ and $P(i|i)$ equal to $P^{(j)}(i|i)$, and the filter-smoother continues with the incremented value for i.

At the last iteration of the filter-smoother, the values of H_i, ν_i, $\Phi(i,i-1)$, and K_i are used in the fixed-point smoother. In order to initialize this part of the algorithm, the matrix D_0 with dummy variables is set equal to $P(0|0)$. Then

$$D_i = D_{i-1}\,\Phi^{T}(i,i-1)\,(I - K_i H_i)^{T} \qquad \text{(B9)}$$

$$\hat{x}^{*}(0|i) = \hat{x}^{*}(0|i-1) + D_i H_i^{T} R^{-1} \nu_i \qquad \text{(B10)}$$

$$P(0|i) = P(0|i-1) - D_i H_i^{T} R^{-1}\,\Phi(i,i-1)\,H_i D_{i-1}^{T} \qquad \text{(B11)}$$

REFERENCES

1. Gerlach, O. H.: Measurement of Performance, Stability and Control Characteristics in Non-Steady Flight With a High-Accuracy Instrumentation System. Rep. VTH-136, Dep. Aeronaut. Eng., Technol. Univ. Delft (Netherlands), Feb. 1966.

2. Mulder, J. A.: Estimation of the Aircraft State in Non-Steady Flight. Methods for Aircraft State and Parameter Identification, AGARD-CP-172, May 1975, pp. 19-1 - 19-21.

3. Jonkers, Herman Louis: Application of the Kalman Filter to Flight Path Reconstruction From Flight Test Data Including Estimation of Instrumental Bias Error Corrections. Ph. D. Thesis, Technol. Univ. Delft (Netherlands), 1976.

4. Wingrove, Rodney C.: Quasi-Linearization Technique for Estimating Aircraft States From Flight Data. J. Aircr., vol. 10, no. 5, May 1973, pp. 303-307.

5. Eulrich, Bernard J.; and Weingarten, Norman C.: Identification and Correlation of the F-4E Stall/Post-Stall Aerodynamic Stability and Control Characteristics From Existing Test Data. AFFDL-TR-73-125, U.S. Air Force, Aug. 1973. (Available from DDC as AD 779 928.)

6. Chen, Robert T. N.; Eulrich, Bernard; and Lebacqz, J. Victor: Development of Advanced Techniques for the Identification of V/STOL Aircraft Stability and Control Parameters. Rep. No. BM-2820-F-1 (Contract N00019-69-C-0534), Cornell Aeronaut. Lab., Inc., Aug. 1971.

7. Etkin, Bernard: Dynamics of Flight. John Wiley & Sons, Inc., c.1959.

8. Bendat, Julius S.; and Piersol, Allan G.: Measurement and Analysis of Random Data. John Wiley & Sons, Inc., c.1966.

9. Klein, V.: On the Adequate Model for Aircraft Parameter Estimation. Rep. Aero No. 28, Cranfield Inst. Technol., Mar. 1975.

TABLE I.- STANDARD ERRORS OF SIMULATED MEASUREMENT NOISE

Variable	Standard error σ of measurement noise of variable
a_x, m/sec^2 . . .	0.02
a_y, m/sec^2 . . .	0.02
a_z, m/sec^2 . . .	0.10
p, rad/sec . . .	0.0008
q, rad/sec . . .	0.0008
r, rad/sec . . .	0.0008
V, m/sec	0.20
β_v, rad	0.0002
α_v, rad	0.0008
φ, rad	0.0008
θ, rad	0.0008

TABLE II.- ELEMENTS OF AUGMENTED STATE VECTOR AND INITIAL ESTIMATES OF AUGMENTED STATE VARIABLE VARIANCES FOR SIMULATED DATA

Augmented state variable	Initial estimate of variance of variable (a)
u, m/sec	1.0
v, m/sec	1.0
w, m/sec	1.0
φ, rad	0.00002
θ, rad	0.00002
b_{ax}, m/sec^2	0.10
b_{ay}, m/sec^2	0.10
b_{az}, m/sec^2	0.10
b_p, rad/sec	0.00005
b_q, rad/sec	0.00005
b_r, rad/sec	0.00005
b_V, m/sec	0.10
b_β, rad	0.0001
b_α, rad	0.0001
b_φ, rad	0.0001
b_θ, rad	0.0001
λ_V	0.00001
λ_β	0.00001
λ_α	0.00001

[a]Main diagonal elements of $P(0|0)$.

TABLE III.- EFFECT OF PROCESS-NOISE COVARIANCE MATRIX FORM ON PARAMETER ESTIMATES FOR SIMULATED DATA

Parameter	True value	Estimate of parameter (a)	
		Case 1 Q = Constant	Case 2 Q = Q(t)
b_{ax}, m/sec^2 . . .	0.20	0.665 (0.0032)	0.25 (0.045)
b_{ay}, m/sec^2 . . .	0.20	0.215 (0.0038)	0.30 (0.15)
b_{az}, m/sec^2 . . .	1.0	0.505 (0.0045)	0.96 (0.15)
b_p, rad/sec . . .	0.004	0.00407 (0.000018)	0.0040 (0.0010)
b_q, rad/sec . . .	0.004	0.00327 (0.000022)	0.0033 (0.00089)
b_r, rad/sec . . .	0.004	0.00428 (0.000014)	0.0042 (0.00090)
b_V, m/sec	2.0	1.75 (0.057)	1.89 (0.29)
b_β, rad	0.002	-0.01620 (0.000084)	0.0084 (0.0030)
b_α, rad	0.01	0.00628 (0.00010)	0.010 (0.0032)
b_φ, rad	0.01	0.0143 (0.00013)	0.0090 (0.0032)
b_θ, rad	0.01	0.00849 (0.000085)	0.010 (0.0026)
λ_V	0.10	0.1027 (0.00049)	0.10 (0.0027)
λ_β	0.10	0.0306 (0.00032)	0.097 (0.0031)
λ_α	0.10	0.1107 (0.00022)	0.10 (0.0028)

[a]Numbers in parentheses are Cramer-Rao lower bounds on standard errors.

TABLE IV.- EFFECT OF INITIAL VALUES OF UNKNOWN PARAMETERS AND REDUCED NUMBER OF UNKNOWNS ON PARAMETER ESTIMATES FOR SIMULATED DATA

Parameter	True value	Estimate of parameter (a)		
		Case 3		Case 4
		1st computer pass	5th computer pass	
b_{ax}, m/sec^2 . . .	0.20	-0.36 (0.047)	0.081 (0.046)	------
b_{ay}, m/sec^2 . . .	0.20	0.78 (0.16)	0.67 (0.15)	0.23 (0.18)
b_{az}, m/sec^2 . . .	1.0	1.42 (0.16)	1.14 (0.15)	------
b_p, rad/sec . . .	0.004	0.0059 (0.0010)	0.0046 (0.0010)	0.0038 (0.00099)
b_q, rad/sec . . .	0.004	0.0030 (0.00087)	0.0032 (0.00088)	------
b_r, rad/sec . . .	0.004	0.0044 (0.00089)	0.0047 (0.00090)	0.0035 (0.00096)
b_V, m/sec	2.0	1.74 (0.29)	3.10 (0.29)	------
b_β, rad	0.002	0.0024 (0.0027)	0.0049 (0.0027)	0.0052 (0.0029)
b_α, rad	0.01	0.022 (0.0029)	0.011 (0.0031)	------
b_φ, rad	0.01	0.0060 (0.0031)	0.0078 (0.0032)	0.0094 (0.0032)
b_θ, rad	0.01	0.0065 (0.0026)	0.0097 (0.0026)	------
λ_V	0.1	0.034 (0.0026)	0.084 (0.0027)	------
λ_β	0.1	0.0003 (0.0031)	0.0011 (0.0031)	0.0002 (0.0031)
λ_α	0.1	0.027 (0.0027)	0.073 (0.0027)	------

[a]Numbers in parentheses are Cramer-Rao lower bounds on standard errors.

TABLE V.- ESTIMATES AND SENSITIVITIES OF PARAMETERS

FROM FOUR COMPUTER PASSES FOR FLIGHT DATA

Parameter	1st computer pass	2nd computer pass		4th computer pass	
	Estimate of parameter (a)	Estimate of parameter (a)	Sensitivity of parameter	Estimate of parameter (a)	Sensitivity of parameter
b_{ax}, m/sec^2 . . .	-0.063 (0.031)	-0.063 (0.028)	5.0	-0.065 (0.019)	12.3
b_{az}, m/sec^2 . . .	0.0012 (0.081)	0.0016 (0.079)	0.0004	-------	----
b_q, rad/sec . . .	-0.00007 (0.00088)	-0.00007 (0.00086)	0.006	-------	----
b_v, m/sec	-0.060 (0.087)	-0.076 (0.080)	1.5	-0.134 (0.076)	8.2
b_α, rad	0.0023 (0.0024)	0.0024 (0.0023)	1.7	0.0022 (0.0021)	1.8
b_θ, rad	0.0003 (0.0022)	0.0004 (0.0021)	0.07	--------	----
λ_v	0.0031 (0.0022)	0.0019 (0.0021)	1.7	0.0047 (0.0018)	18.2
λ_α	0.0019 (0.0031)	0.0021 (0.0031)	0.43	0.0041 (0.0031)	1.7

[a]Numbers in parentheses are Cramer-Rao lower bounds on standard errors.

TABLE VI.- INITIAL AND SMOOTHED VALUES OF STATE VARIABLES AND VARIANCES FROM THREE COMPUTER PASSES FOR FLIGHT DATA

State variable	Pass no.	Estimate of variable		Variance of variable	
		Initial value, $\hat{x}(0\|0)$	Smoothed value, $\hat{x}(0\|N)$	Initial value (a)	Smoothed value (b)
u, m/sec . . .	1	46.174	46.09	0.01	0.0076
w, m/sec . . .	1	2.368	2.37	0.01	0.0083
θ, rad	1	0.03941	0.0394	0.000001	0.00000095
u, m/sec . . .	3	46.174	46.16	0.0076	0.0064
w, m/sec . . .	3	2.368	2.37	0.0083	0.0080
θ, rad	3	0.03941	0.0394	0.00000095	0.00000094

[a]Main diagonal elements of $P(0|0)$.
[b]Main diagonal elements of $P(0|N)$.

TABLE VII.- PARAMETER AND STANDARD ERROR ESTIMATES

FROM EIGHT FLIGHT-DATA RUNS

Run no.	$\hat{b}_{ax}$, m/sec^2	$\hat{b}_{ay}$, m/sec^2	$\hat{b}_{az}$, m/sec^2	$\hat{b}_{r}$, rad/sec	$\hat{b}_{\beta}$, rad	$\hat{b}_{\alpha}$, rad	$\hat{b}_{\varphi}$, rad	$\hat{b}_{\theta}$, rad	$\hat{\lambda}_{V}$	$\hat{\lambda}_{\beta}$
1	-0.076	0.099	-0.073	-0.0023	-0.0010	-0.0022	0.0007	0.0028	0.0016	-0.0908
2	-.065	.113	-.076	-.0024	-.008	-.0024	.0017	.0022	.0014	-.0908
3	-.049	.116	-.079	-.0025	-.0029	-.0025	.0013	.0016	.0007	-.0904
4	-.078	.124	-.084	-.0025	-.0008	-.0017	.0014	.0030	.0025	-.0907
5	-.108	.140	-.095	-.0032	-.0009	-.0050	.0013	.0036	.0023	-.0904
6	-.079	.147	-.102	-.0033	-.0013	-.0053	.0017	.0024	.0020	-.0903
7	-.063	.138	-.109	-.0036	.0060	-.0025	.0004	.0020	.0037	-.0898
8	-.084	.124	-.098	-.0035	-.0012	-.0026	.0006	.0031	.0002	-.0900
Average standard error of b_y	0.021	0.052	0.060	0.00075	0.0017	0.0019	0.0018	0.0015	0.0012	0.0022

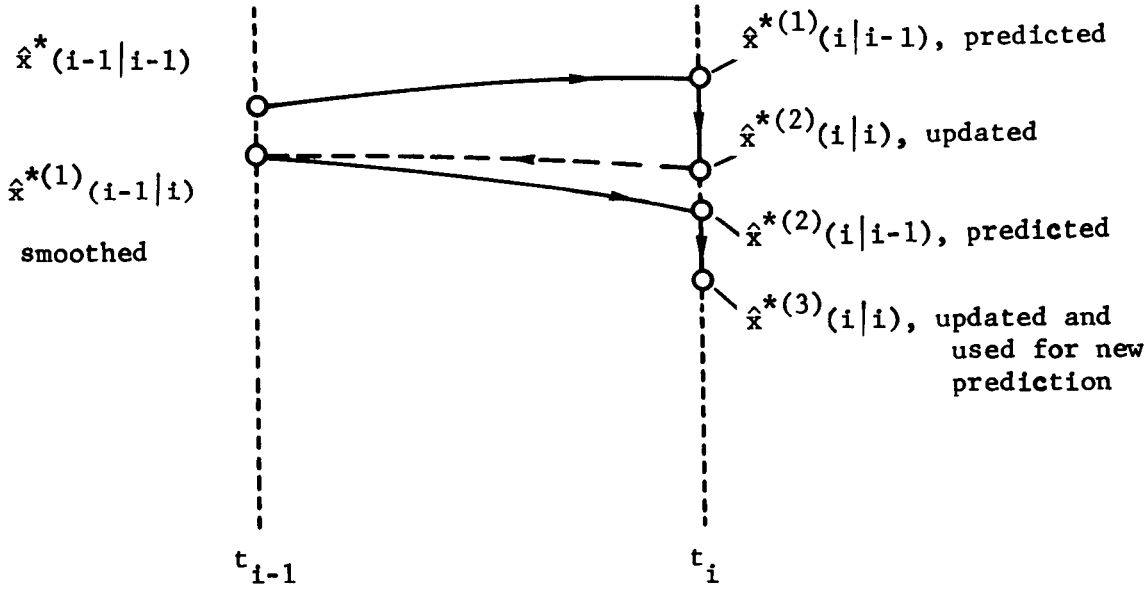

Figure 1.- Computing scheme for two iterations of extended Kalman filter-smoother.

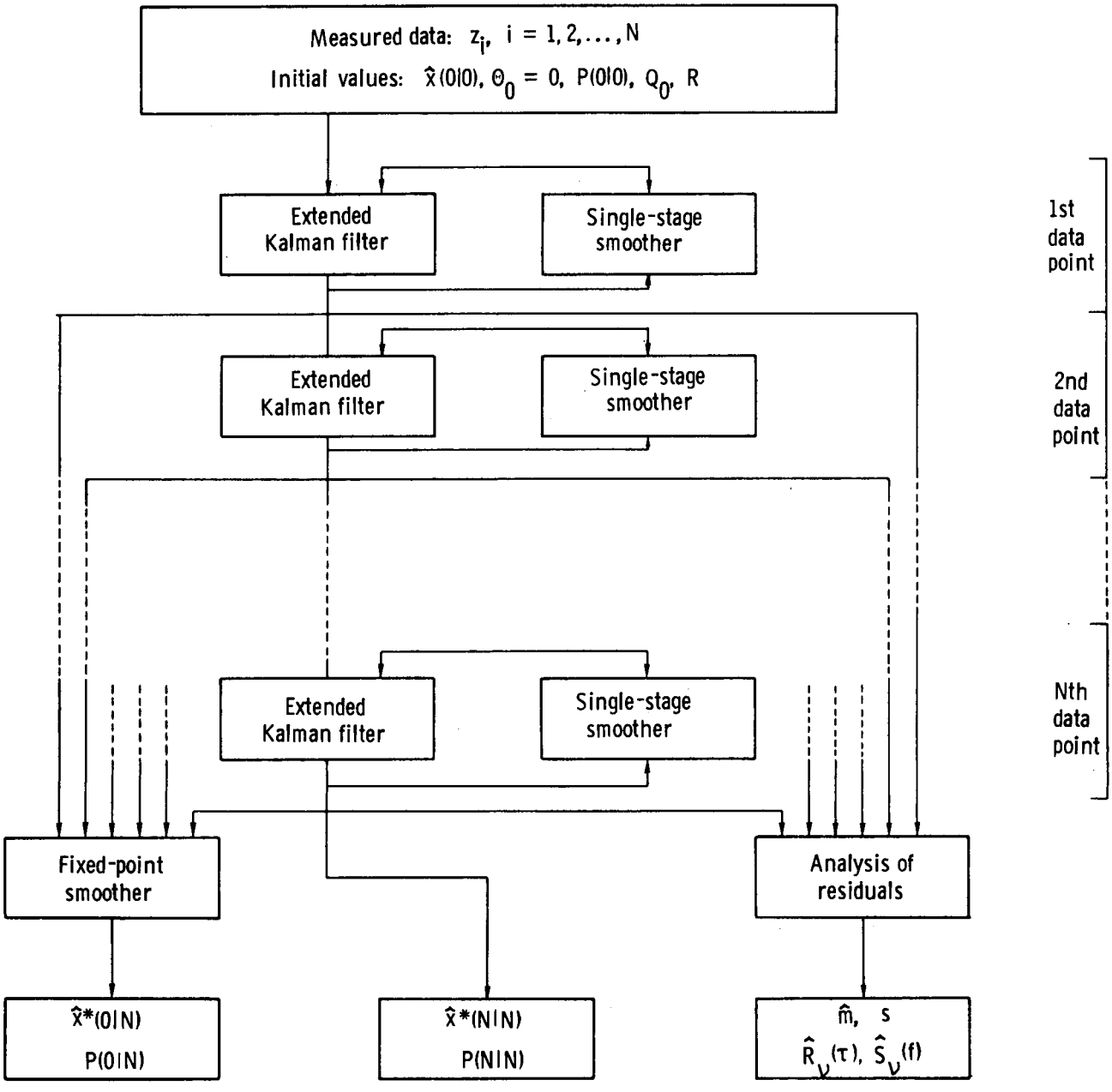

Figure 2.- Block diagram of identification process.

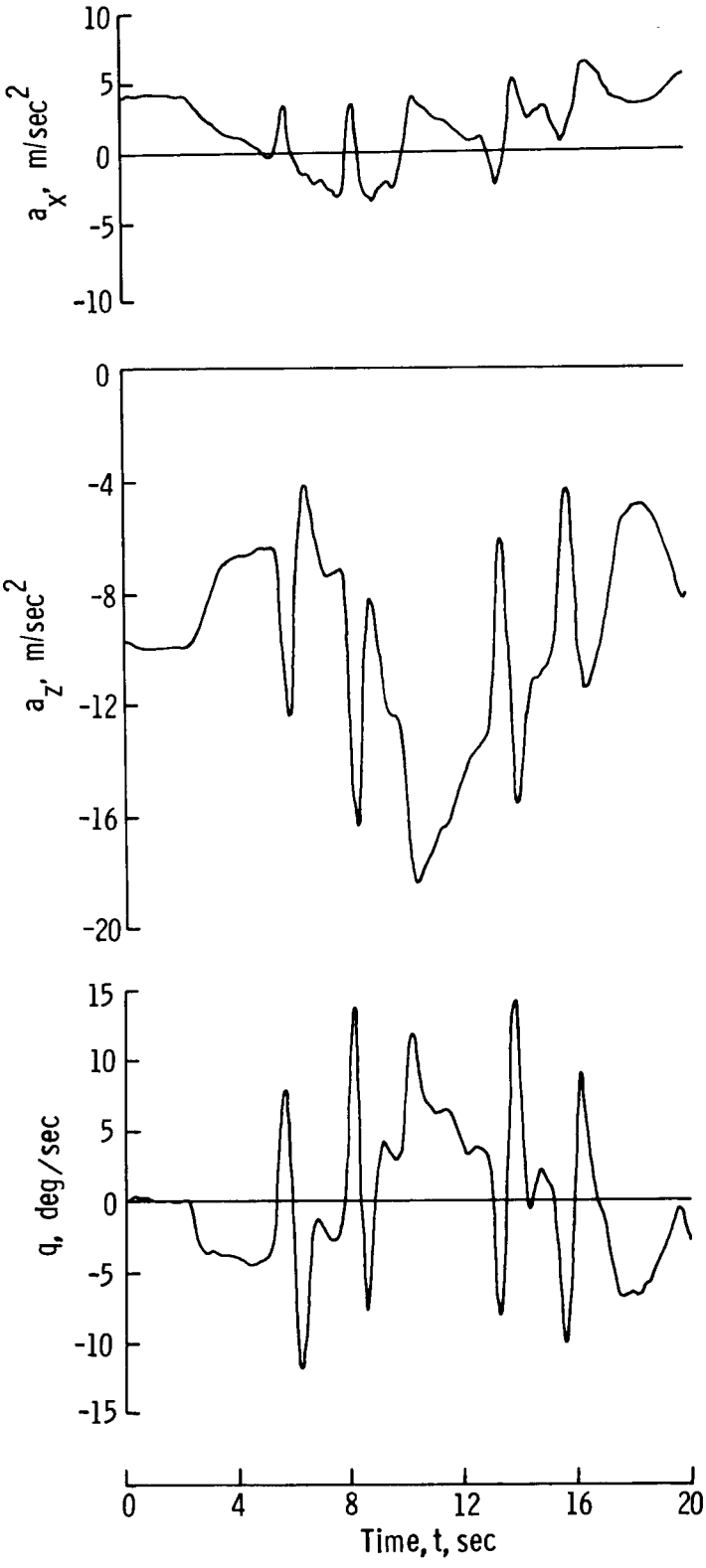

Figure 3.- Time histories of measured input and output variables for three-degree-of-freedom longitudinal motion.

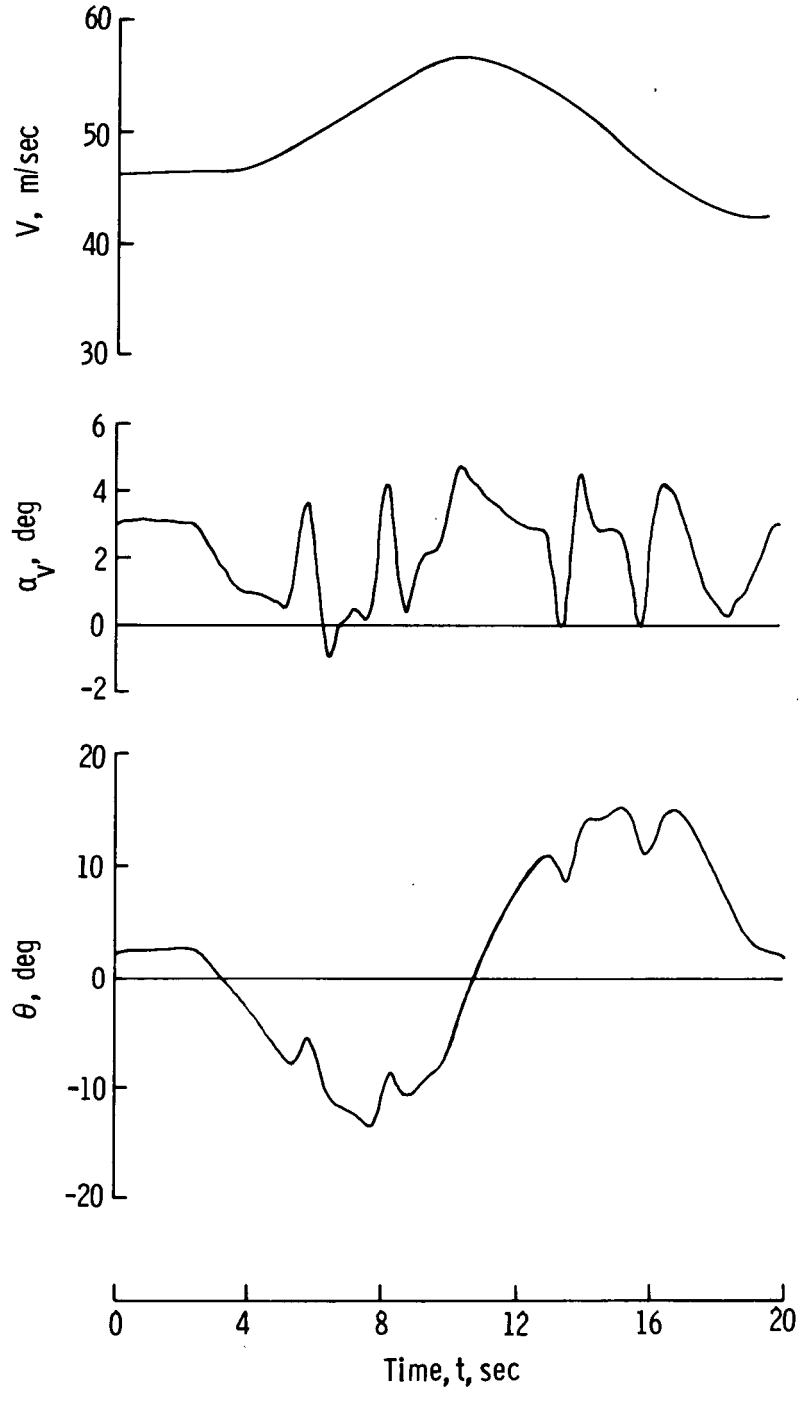

Figure 3.- Concluded.

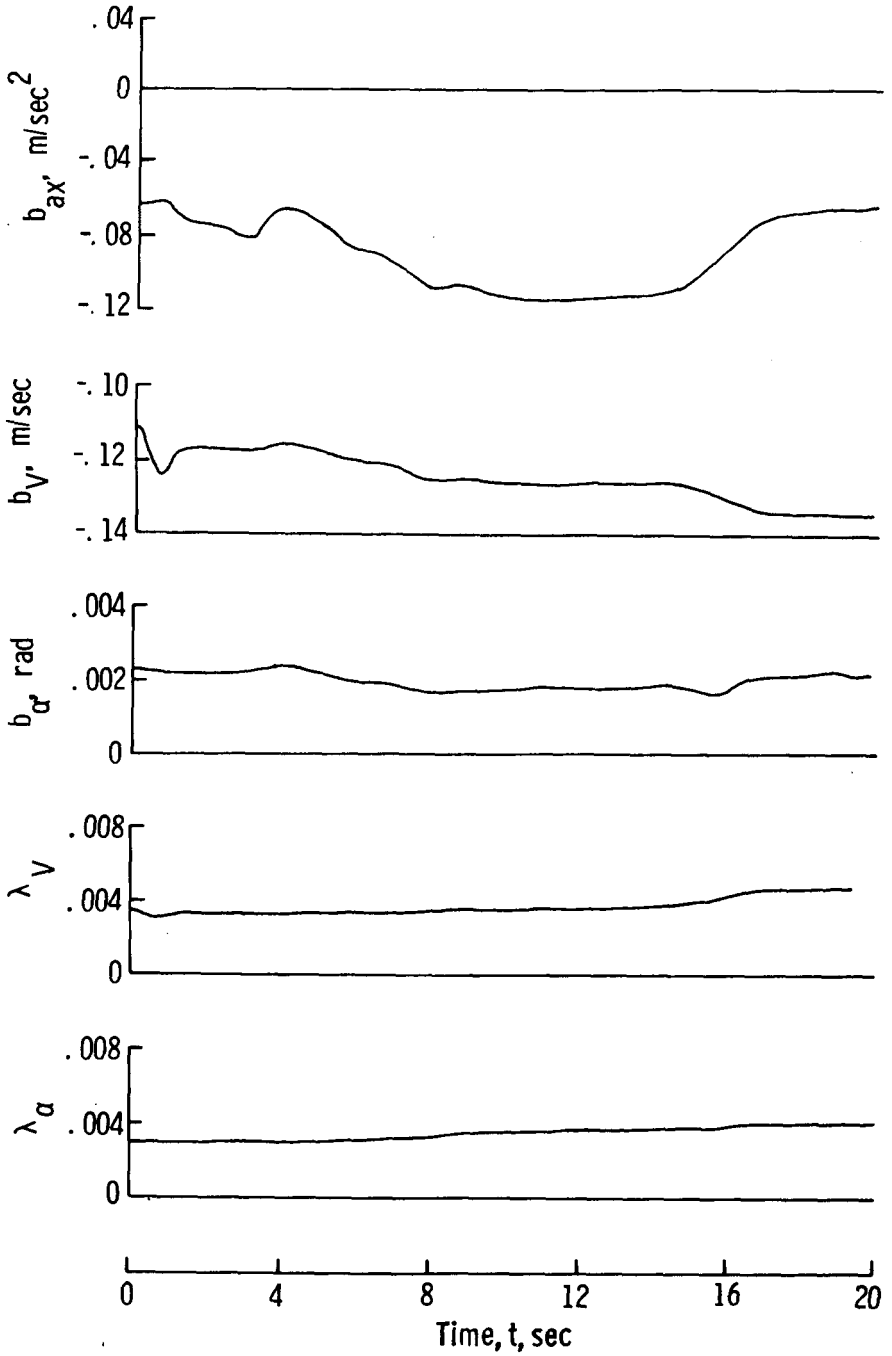

Figure 4.- Time histories of estimated parameters. 4th computer pass; three-degree-of-freedom longitudinal motion.

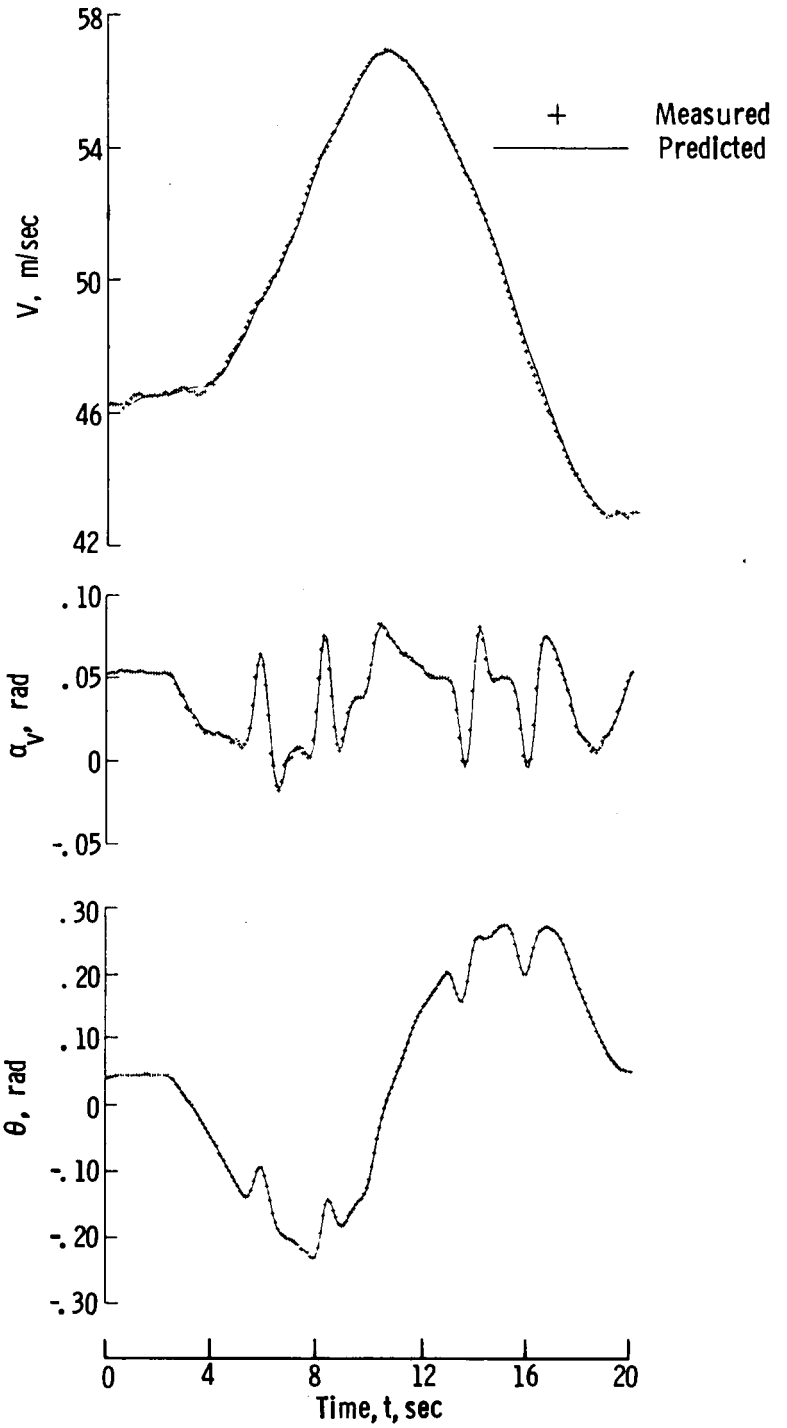

Figure 5.- Comparison of measured and predicted time histories of output variables. Three-degree-of-freedom longitudinal motion.

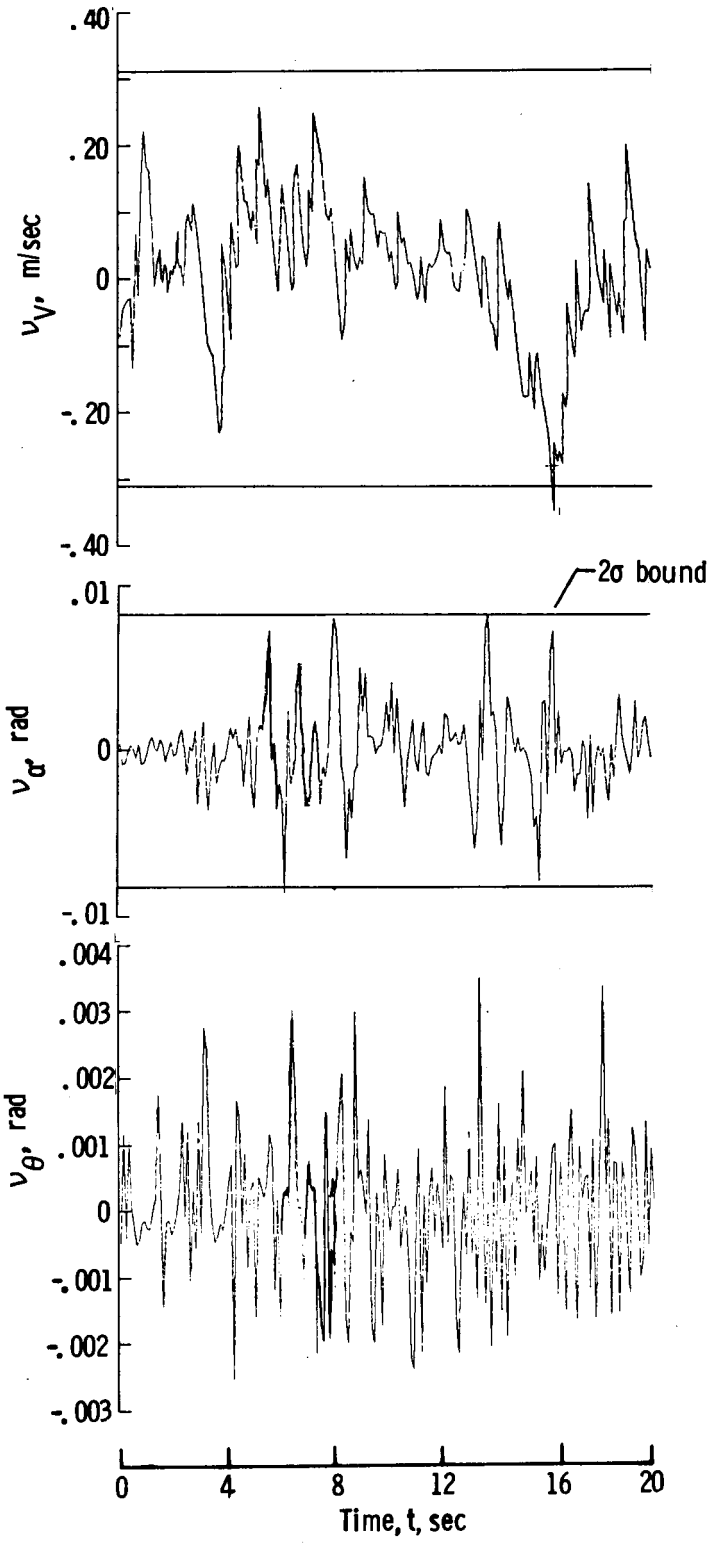

Figure 6.- Time histories of residuals. Three-degree-of-freedom longitudinal motion.

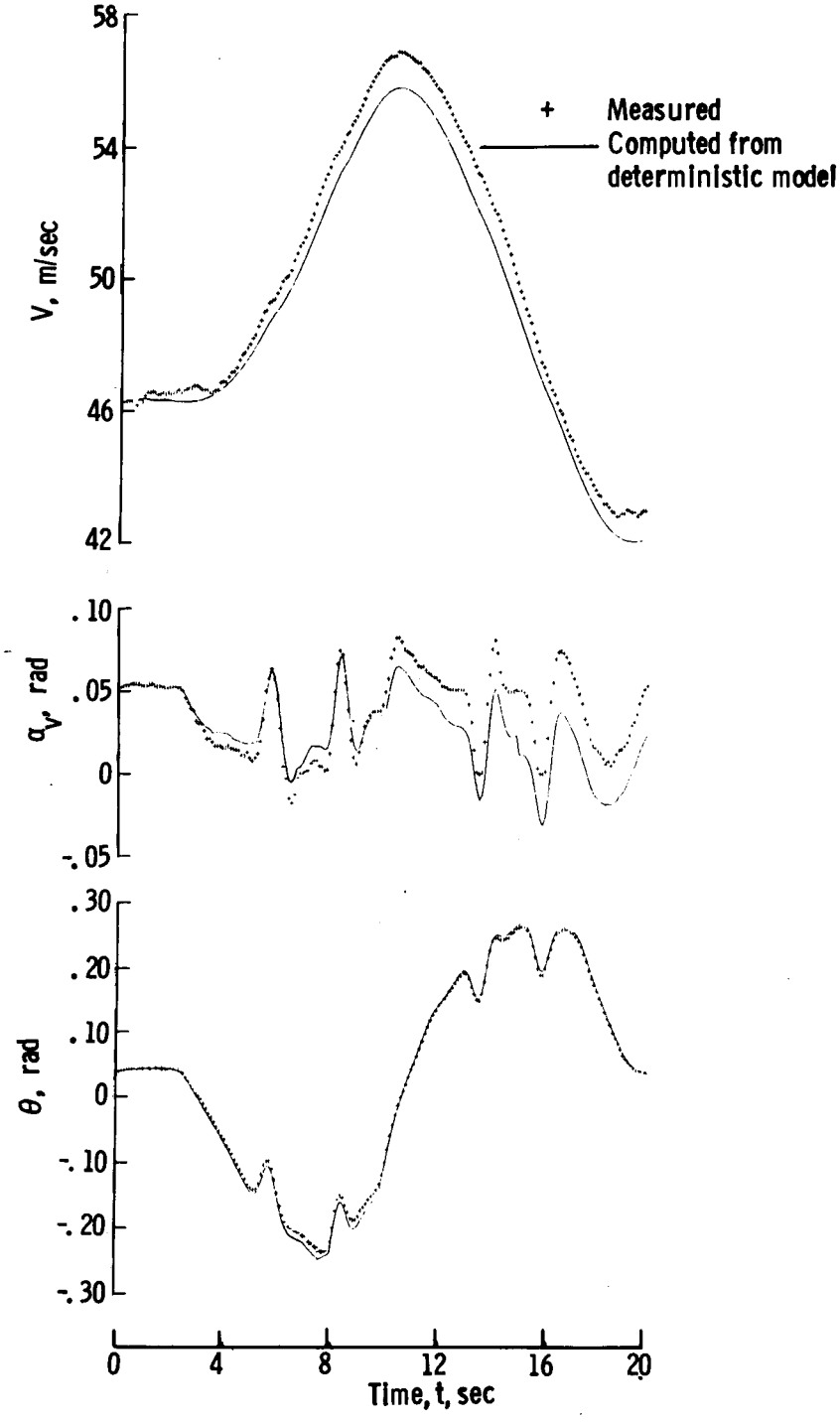

Figure 7.- Measured and computed time histories of output variables from deterministic model. Three-degree-of-freedom longitudinal motion.

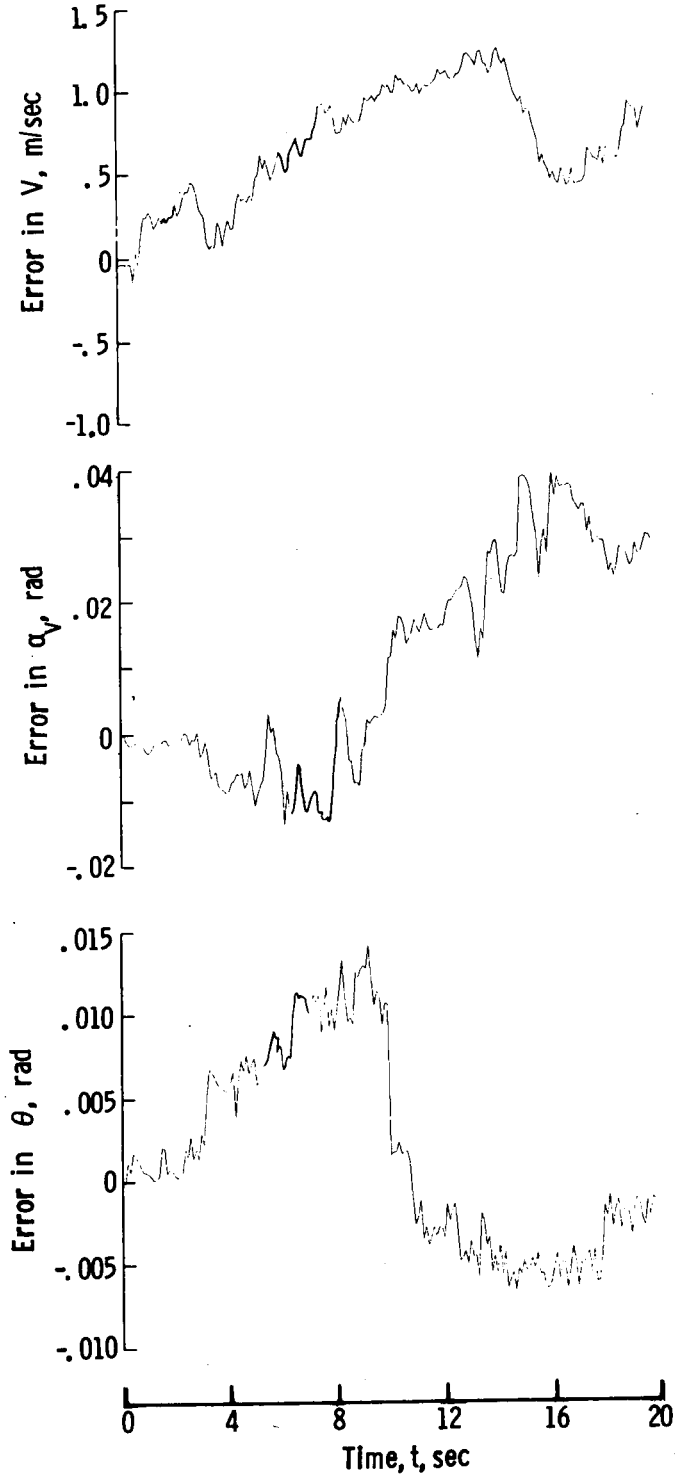

Figure 8.- Time histories of errors in output variables from deterministic model. Three-degree-of-freedom longitudinal motion.

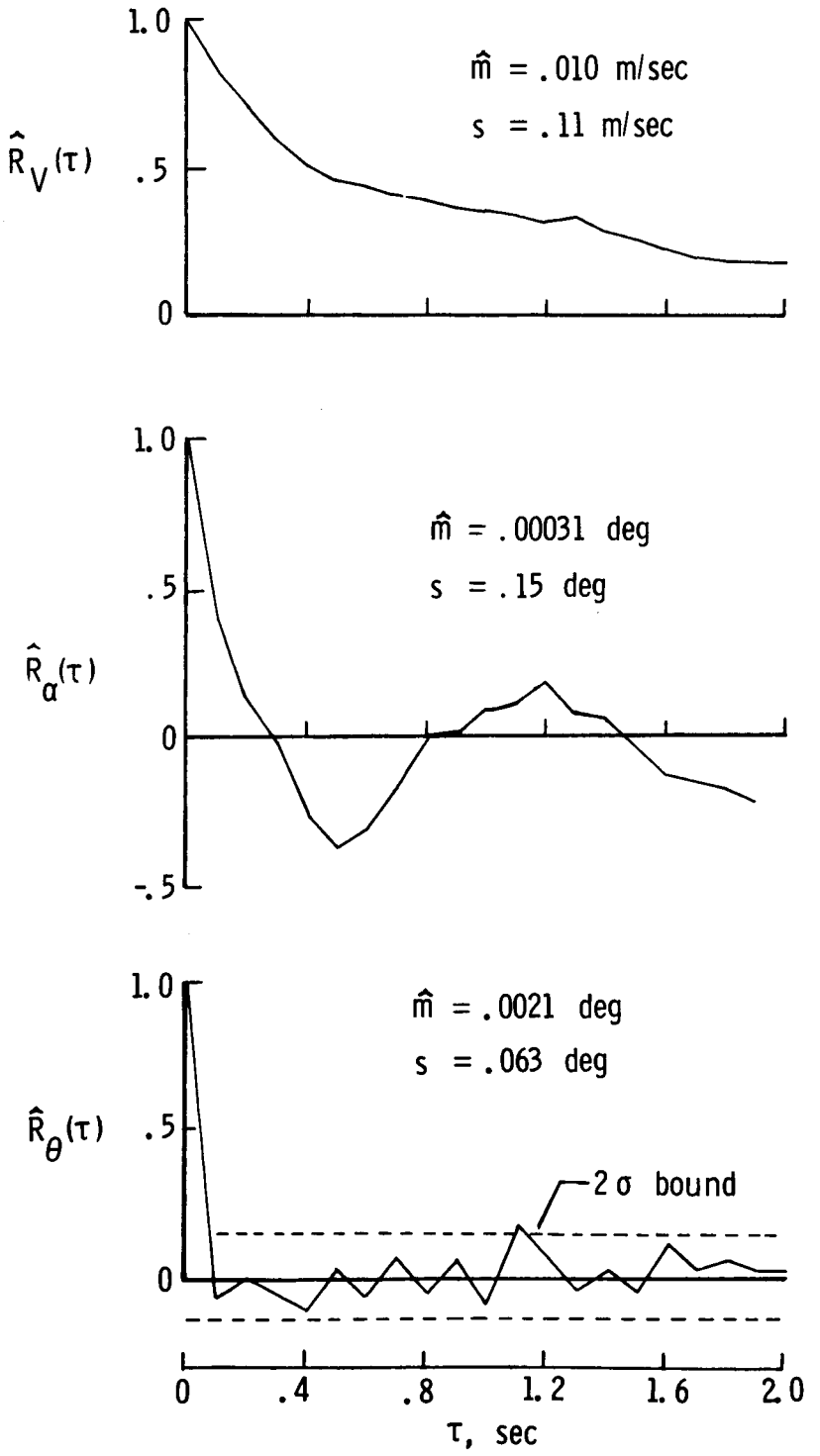

Figure 9.- Mean values, standard errors, and autocorrelation functions of residuals. Three-degree-of-freedom longitudinal motion.

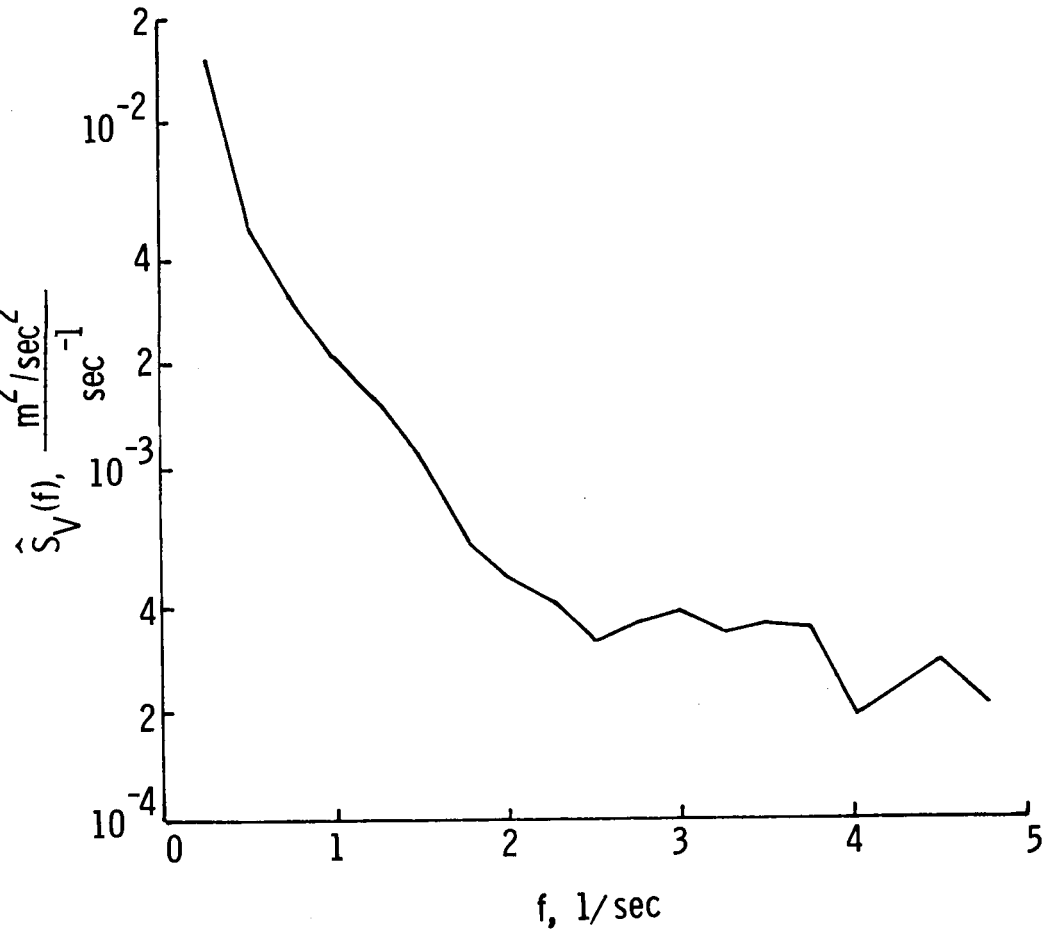

Figure 10.- Power spectral densities of residuals. Three-degree-of-freedom longitudinal motion.

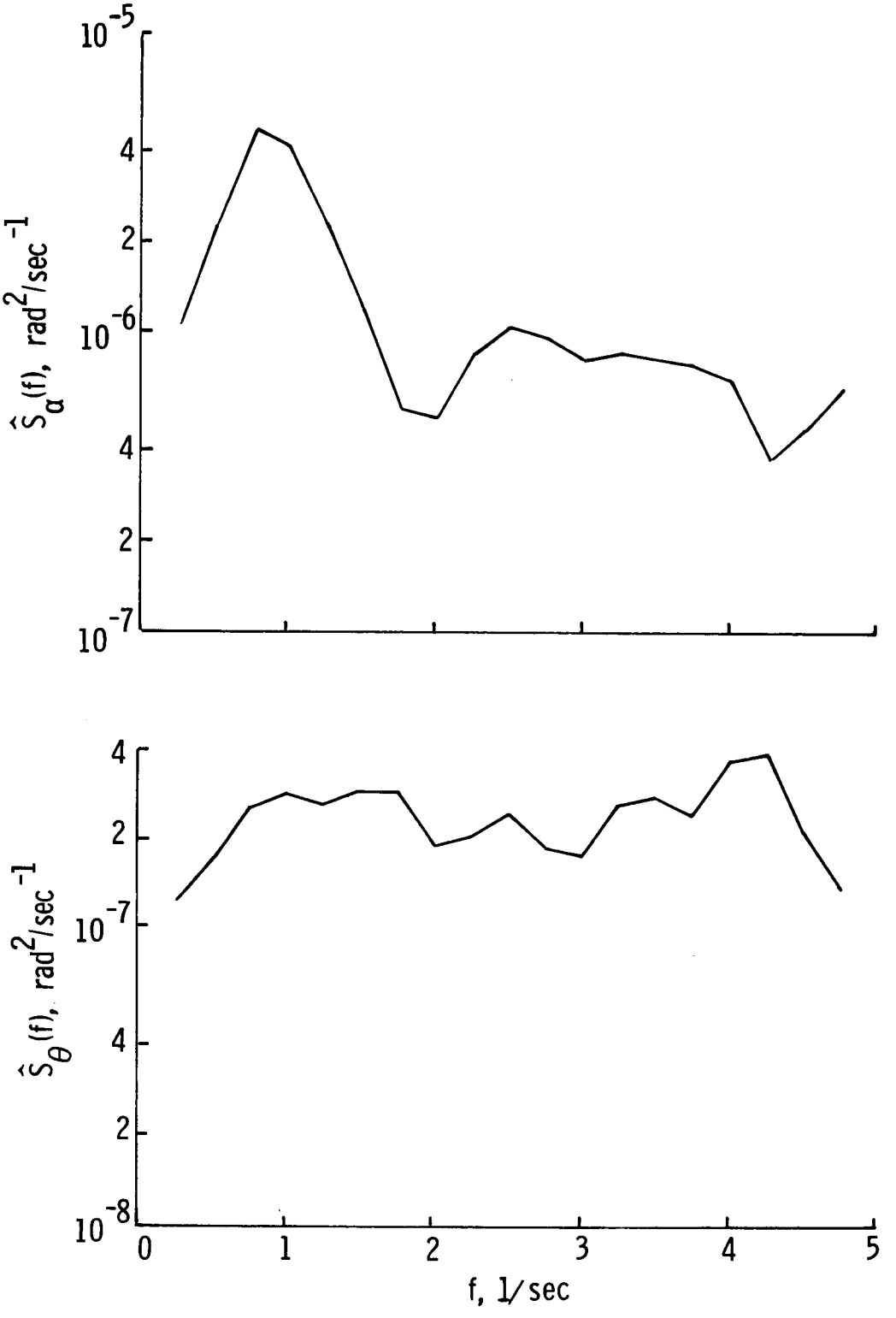

Figure 10.- Concluded.

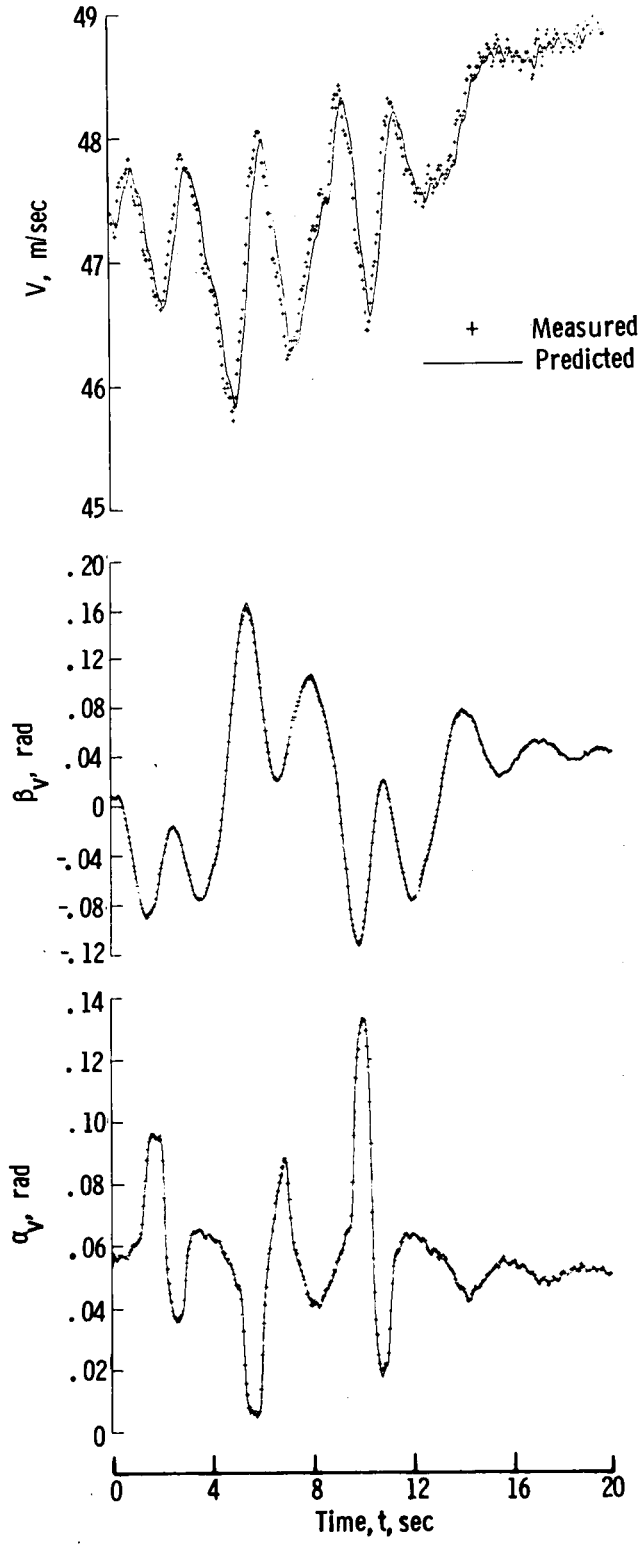

Figure 11.- Comparison of measured and predicted time histories of output variables for six-degree-of-freedom motion. Flight-data run 5.

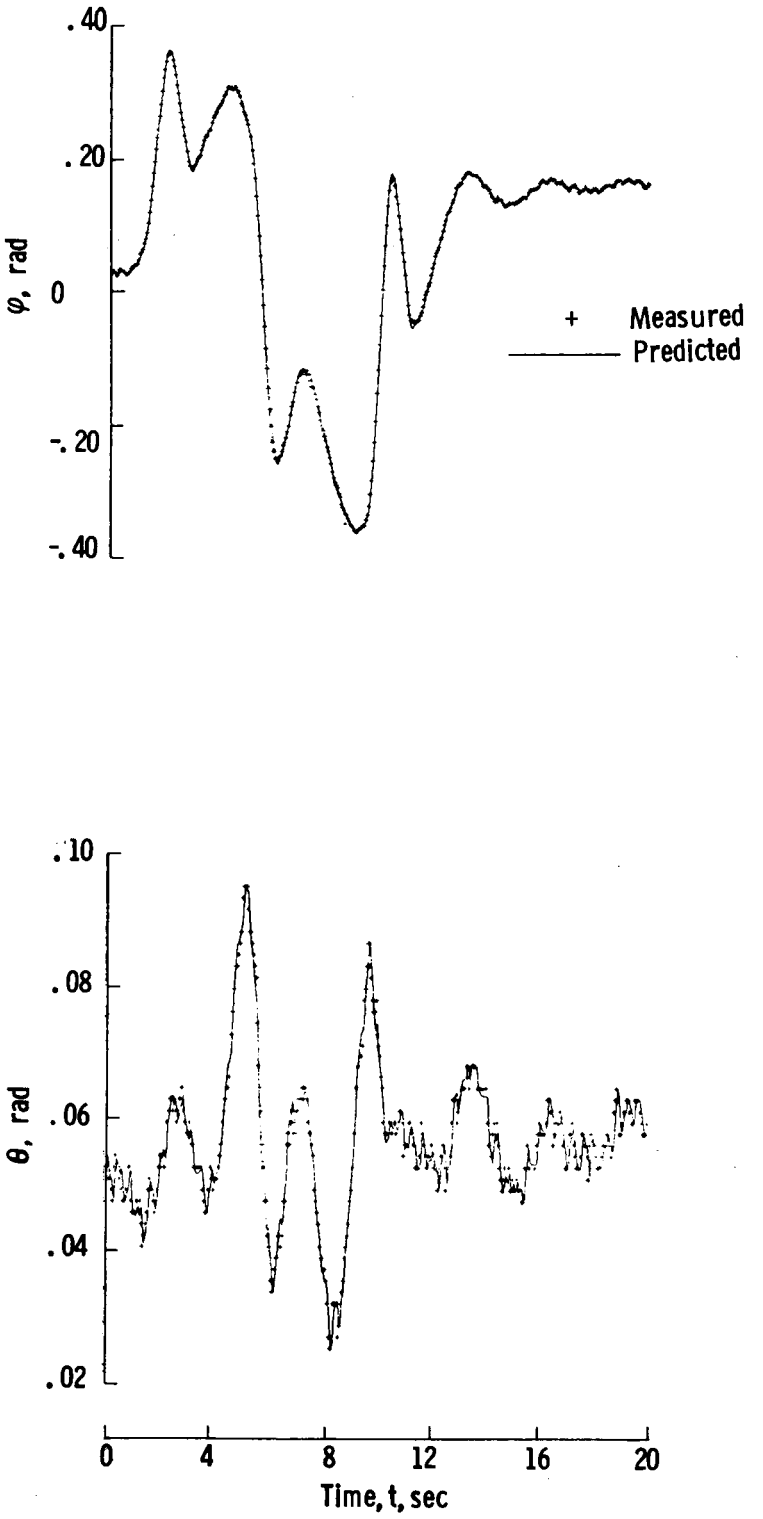

Figure 11.- Concluded.

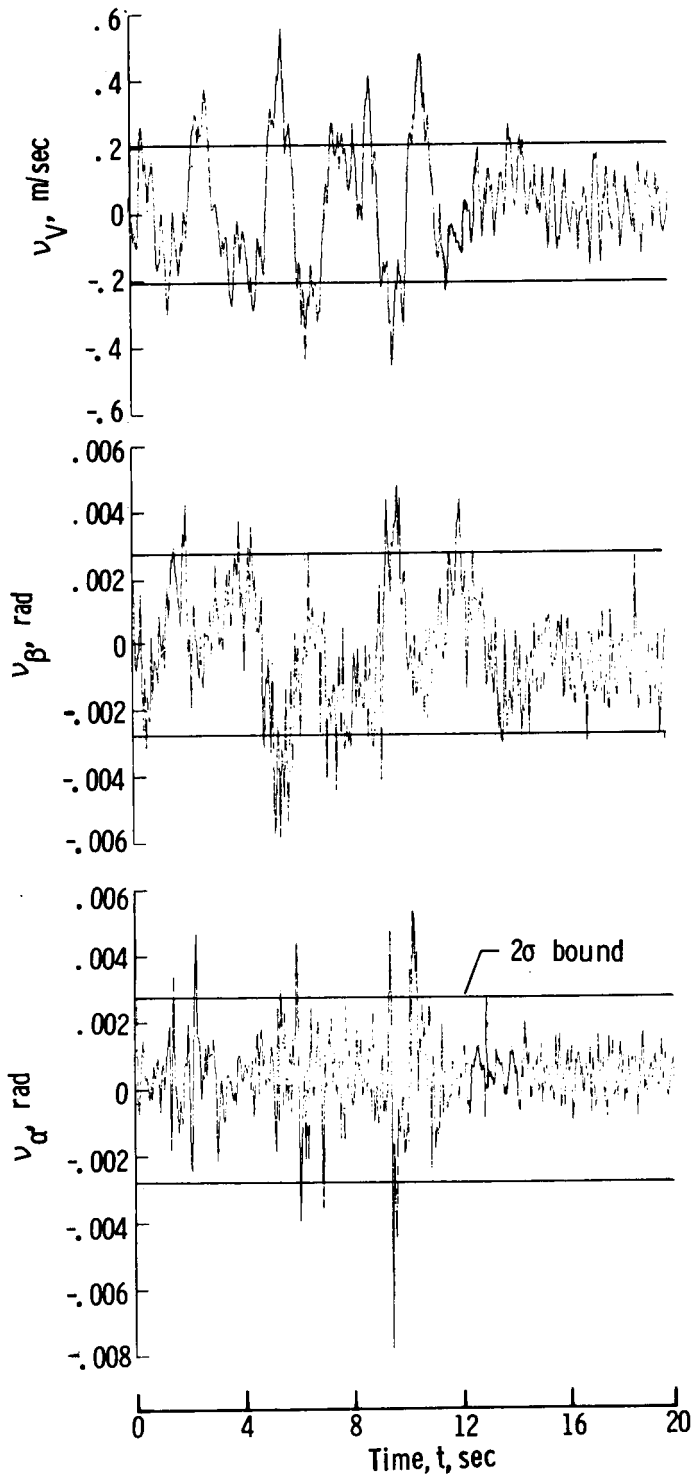

Figure 12.- Time histories of residuals. Six-degree-of-freedom motion; flight-data run 5.

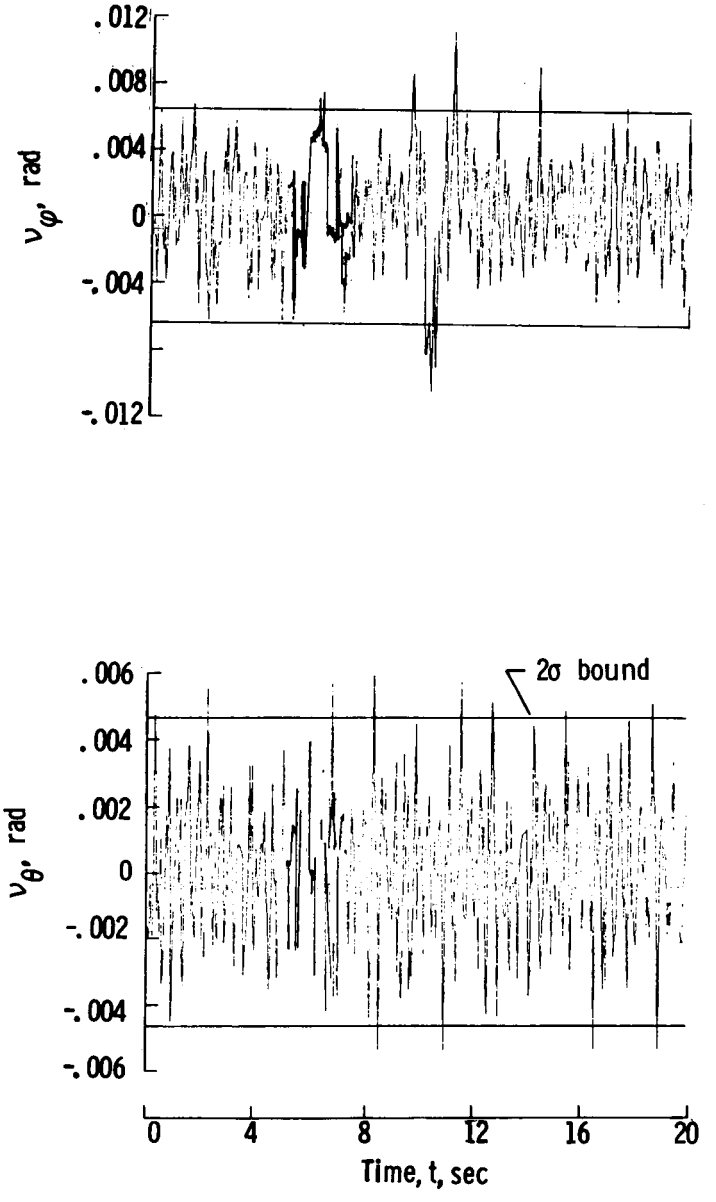

Figure 12.- Concluded.

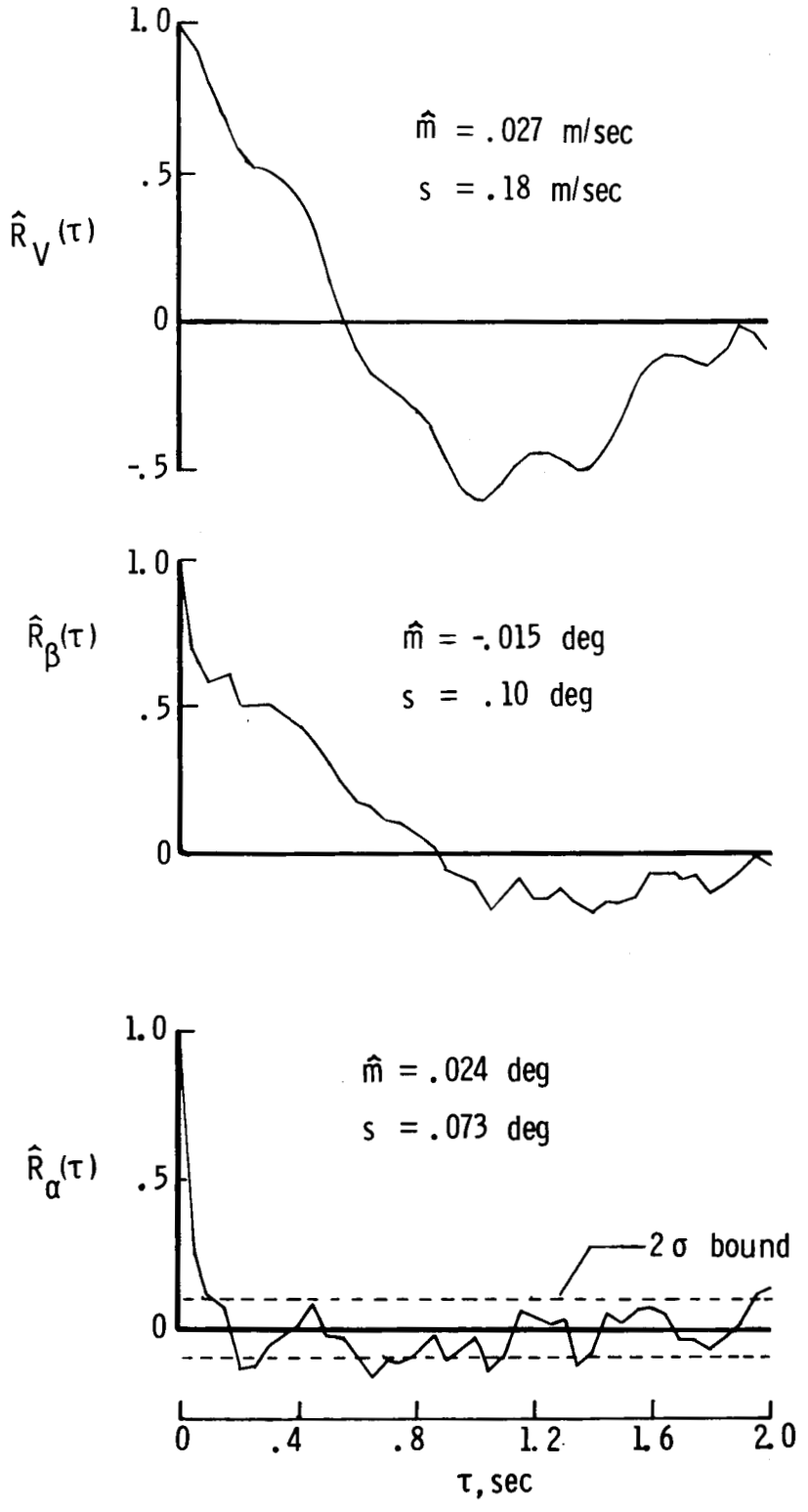

Figure 13.- Mean values, standard errors, and autocorrelation functions of residuals. Six-degree-of-freedom motion; flight-data run 5.

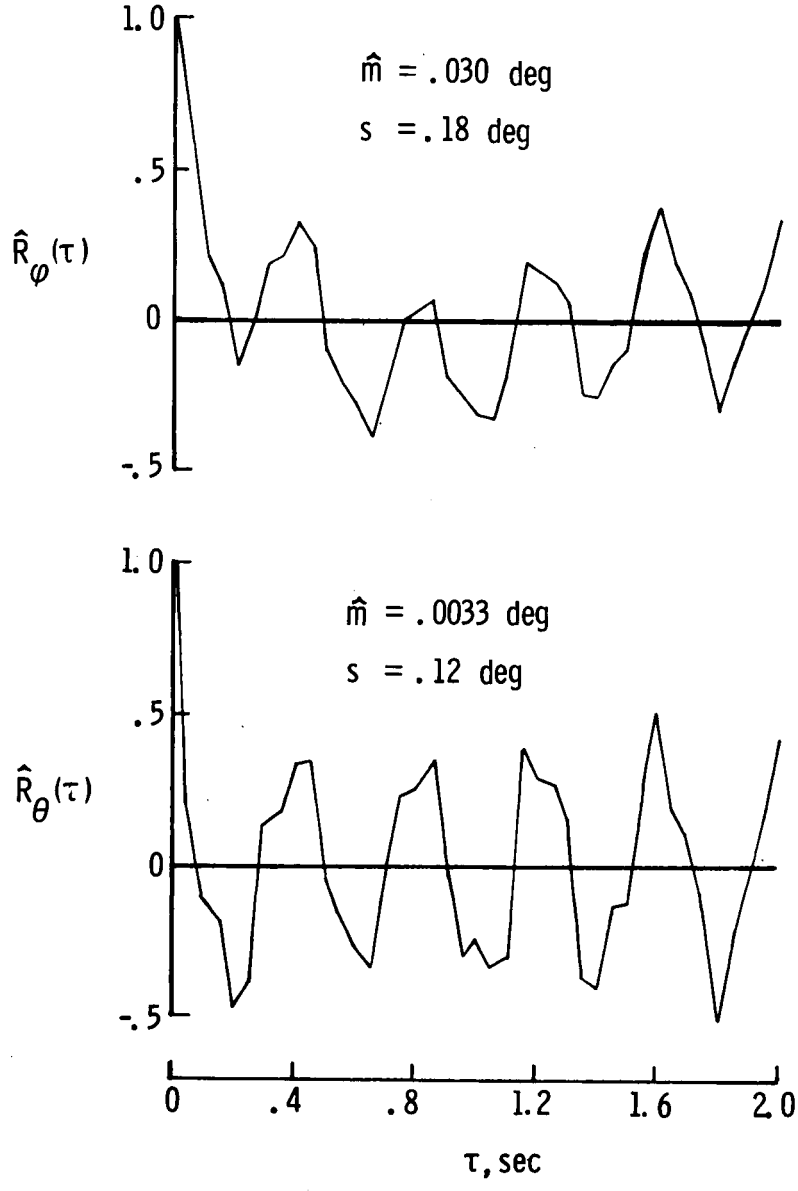

Figure 13.- Concluded.

1. Report No.	2. Government Accession No.	3. Recipient's Catalog No.
NASA TN D-8514		

4. Title and Subtitle	5. Report Date
COMPATIBILITY CHECK OF MEASURED AIRCRAFT RESPONSES USING KINEMATIC EQUATIONS AND EXTENDED KALMAN FILTER	August 1977
	6. Performing Organization Code

7. Author(s)	8. Performing Organization Report No.
Vladislav Klein and James R. Schiess	L-11420
	10. Work Unit No. 505-06-93-01
9. Performing Organization Name and Address NASA Langley Research Center Hampton, VA 23665	11. Contract or Grant No.
	13. Type of Report and Period Covered Technical Note
12. Sponsoring Agency Name and Address National Aeronautics and Space Administration Washington, DC 20546	14. Sponsoring Agency Code

15. Supplementary Notes

Vladislav Klein: The George Washington University, Joint Institute for Advancement of Flight Sciences.

James R. Schiess: Langley Research Center.

16. Abstract

An extended Kalman filter-smoother and a fixed-point smoother are used for estimation of the state variables in the six-degree-of-freedom kinematic equations relating measured aircraft responses and for estimation of unknown constant bias and scale factor errors in measured data. In addition to a compatibility check of measured responses and estimation of bias errors, the computing algorithm includes an analysis of residuals which can improve the filter performance and provide estimates of measurement noise characteristics for some aircraft output variables. The technique developed is demonstrated in several examples using simulated and real flight-test data. Improved accuracy of measured data is obtained when the data are corrected for estimated bias errors.

17. Key Words (Suggested by Author(s))	18. Distribution Statement
Flight-test data analysis	Unclassified - Unlimited Subject Category 05

19. Security Classif. (of this report)	20. Security Classif. (of this page)	21. No. of Pages	22. Price*
Unclassified	Unclassified	47	$4.00

*For sale by the National Technical Information Service, Springfield, Virginia 22161